forecasting

MDPI

Article

Unveiling the Dynamics of Wholesale Sales and Business Cycle Impacts in Japan: An Extended Moving Linear Model Approach

Koki Kyo and Hideo Noda *

Department of Business Economics, School of Management, Tokyo University of Science, 1-11-2 Fujimi, Chiyoda-ku, Tokyo 102-0071, Japan; kyo@rs.tus.ac.jp
* Correspondence: noda@rs.tus.ac.jp

Abstract

Wholesale sales value is one of the key elements included in the coincident indicator series of the indexes of business conditions in Japan. The objectives of this study are twofold. The first is to comprehend features of dynamic structure of various components for 12 business types of the wholesale sales in Japan, focusing on the period from January 1980 to December 2022. The second is to elucidate effect of business cycles on the behavior of each business type of wholesale sales. Specifically, we utilize our moving linear model approach to decompose monthly time-series data of wholesale sales into a seasonal component, an unusually varying component containing outliers, a constrained component, and a remaining component. Additionally, we construct a distribution-free dynamic linear model and examine the time-varying relationship between the decomposed remaining component, which contains cyclical variation, in each business type of the wholesale sales and that in the coincident composite index. Our proposed approach reveals complex dynamics of various components of time series on wholesale sales. Furthermore, we find that different business types of the wholesale sales exhibit diverse responses to business cycles, which are influenced by macroeconomic conditions, government policies, or exogenous shocks.

Keywords: components decomposition; economic time series; dynamic structure; Japanese economy; moving linear model approach; wholesale sales

check for updates

Academic Editor: Vasilios Plakandaras

Received: 2 August 2025
Revised: 21 September 2025
Accepted: 22 September 2025
Published: 26 September 2025

Citation: Kyo, K.; Noda, H. Unveiling the Dynamics of Wholesale Sales and Business Cycle Impacts in Japan: An Extended Moving Linear Model Approach. *Forecasting* **2025**, *7*, 54. https://doi.org/10.3390/forecast7040054

Copyright: © 2025 by the authors. Licensee MDPI, Basel, Switzerland. This article is an open access article distributed under the terms and conditions of the Creative Commons Attribution (CC BY) license (https://creativecommons.org/licenses/by/4.0/).

1. Introduction

Wholesale sales value is one of the key elements included in the coincident indicator series of the indexes of business conditions in Japan. While the significance of wholesale sales is widely recognized, systematic research on the decomposition of time-series data by business type remains limited. Such an approach is essential for uncovering the characteristics of the dynamic structure within the wholesale sector. Another important unresolved issue is the relationship between the various types of wholesale sales and the business cycles. These issues are crucial in deepening our understanding of the significance of including wholesale sales value in the indexes of business conditions.

Although there are numerous instances of data analysis in various socio-economic fields, comparable cases of data analysis within the same field are not commonly observed, with different methods being employed in each instance. For example, ref. [1] conducted an analysis of the impact of sudden events on China's automobile industry stock prices using the incident research method. Ref. [2] examined the validity of including wholesale and retail sales in the coincident indexes of business conditions in Japan. Ref. [3] analyzed

the evolution of the retail sector during the 2019 coronavirus disease (COVID-19) using the Scopus bibliographic database and identified future research issues.

From a methodological perspective on time-series analysis, various approaches have been proposed. Ref. [4] provide a foundation of time-series analysis, forecasting methods, and control techniques. Ref. [5] introduced basic theories and methods for time-series analysis, while the work of [6] serves as a comprehensive guide, introducing readers to modeling techniques used in analyzing sequential data. These references fall within the scope of traditional time-series analysis, primarily dealing with stationary time series. For non-stationary time series, such as those with mean non-stationarity, it is common to take differences to approximately transform the original time series into a stationary form before applying conventional methods. However, there is a drawback in processing time series through differencing, as it leads to a loss of information contained in the original data. Therefore, methods have been proposed to decompose the original time series into several components, separating stationary and non-stationary components (see, e.g., [7]; see also [8]). Moreover, ref. [9] introduced a method of autoregressive modeling with time-varying coefficients to analyze autocorrelation non-stationary time series. Ref. [10] analyzed the dynamics of oil and food prices using the bootstrapped time-varying Granger causality method by [11] to identify and examine date-stamp causal changes in the predictive effects between oil and food markets. Note that Kitagawa–Gersch's approaches may not function effectively depending on the nature of the data. For instance, ref. [7] sometimes faced challenges in successfully separating cyclical components (see, e.g., [12]). Furthermore, existing approaches often rely on strict assumptions about the distribution of the data, such as normality, homoscedasticity, and heteroscedasticity assumptions. To address these issues, Ref. [13] proposed the moving linear (ML) model approach. The distinctive feature of this approach lies in its simplicity and flexibility in modeling, eliminating the need for stringent assumptions about the data distribution.

We consider the monthly time-series data of wholesale sales to be composed of a seasonal component, an unusually varying component containing outliers (representing abnormal variations), a constrained component (representing the trend), and a remaining component (representing cyclical variations). Thus, the purpose of this research is the following two points. The first is to comprehend the dynamic features of various components for 12 business types of wholesale sales in Japan. Specifically, 12 business types of wholesale sales are as follows: General Merchandise, Textiles, Apparel and Accessories, Livestock and Aquatic Products, Food and Beverages, Building Materials, Chemicals, Minerals and Metals, Machinery and Equipment, Furniture and House Furnishings, Medicines and Toiletries, and Others. The second is to elucidate effects of business fluctuations on the behavior of each business type of wholesale sales. The significance of wholesale sales extends beyond economic indicators, providing insights into global movements, societal shifts, and the repercussions of unforeseen events such as economic downturns or natural disasters. The analysis of these sales offers a multifaceted perspective. Therefore, we target the wholesale sector to elucidate structural changes in 12 business types of wholesale sales over time and discern the influences of business fluctuations on the behavior of each business type of wholesale sales.

To achieve the first objective, we employ the ML model approach developed by [13]. In addition, we conduct the anomaly detection and estimation using the method proposed by [14]. These methodologies aid in decomposing each time series into trend, seasonal variation, cyclical patterns, and abrupt fluctuations, allowing for an in-depth investigation into the factors and outcomes influencing each component's variations. Regarding the second objective, we analyze effects of business fluctuations using the coincident composite index (CI) as an index for business cycle analysis. This involves exploring the relationship

between the coincident CI and the cyclical components in wholesale sales of every business type. While recognizing the temporal variability of such relationships, we address this challenge by employing a time-varying coefficient linear model. It should be noted that given the complexity of the error term's probability distribution in such linear models, conventional modeling approaches become challenging. Thus, we propose a distribution-free dynamic linear (DFDL) model approach based on the ML model by [13] and apply it to analyze the dynamic relationships in the second objective, establishing the framework of this study. Our analytical results reveal the complex dynamics of the various components in the time series of wholesale sales value. Additionally, each business type of wholesale sales value responds diversely to business fluctuations, influencing exogenous and serious shocks, such as the global financial crisis and the COVID-19 pandemic.

Furthermore, it is important to recognize that the methods developed and applied in this study inherently possess the capacity for extrapolation in time-series analysis. The constrained component is modeled using a local linear framework, which naturally allows for extrapolation, while the remaining component—although not based on an explicit distributional assumption—can be reasonably treated within an ARMA framework due to its broadly stationary nature. The processes for detecting and estimating outliers are also directly relevant to predictive tasks. While the primary focus of this study has been on elucidating dynamic structures in historical data, the analytical framework and approaches introduced here also offer clear potential for forecasting applications. This perspective highlights that the insights gained from past data can not only inform understanding of historical dynamics but also provide a foundation for predictive studies in wholesale sales and related economic variables.

The remainder of this article is organized as follows. In Section 2, we review related work and provide a detailed overview of our previous research. Section 3 provides a detailed review of our previous research, including the ML model approach and its extended version. Section 4 presents an illustrative example for decomposing time series for the wholesale sales of each business type in Japan and analyzing the dynamics in the decomposed results. In Section 5, we newly introduce a time-varying linear model approach for analyzing the dynamics in the relationship between the cyclical components in wholesale sales of every business type and business fluctuations. Section 6 presents another illustrative example by applying the approach introduced in Section 5. In Section 7, we present a summary and discussion.

2. Related Work and Literature Review

Time-series decomposition and seasonal adjustment have long been central topics in econometrics and statistics. Traditional approaches, such as classical decomposition and ARIMA-based methods, primarily assume stationarity or require transformations (e.g., differencing) to approximate stationarity before applying conventional techniques [4–6] . While these methods provide foundational tools, they can lead to information loss when processing non-stationary time series.

To address non-stationarity, models of Structural Time Series (STS), notably Harvey's framework [15], allow for decomposition into trend, seasonal, and irregular components with time-varying parameters. STS approaches offer greater flexibility than classical methods, but they typically rely on distributional assumptions and require careful specification of model structures. Extensions of STS models include the Bayesian Structural Time Series (BSTS) [16], which incorporates prior information and allow probabilistic inference, and STL decomposition [17], which uses Loess smoothing for flexible seasonal-trend decomposition without strong parametric assumptions. Other widely used approaches

include X-13ARIMA-SEATS [18] for official seasonal adjustment and Kalman-filter-based unobserved component models for extracting latent trends and cycles.

Although these established methods are effective, their application to highly granular wholesale sales data across multiple business types remains limited. Most approaches either require strict distributional assumptions or are designed for single aggregated series, making them less suitable for analyzing diverse and dynamic components in wholesale sales.

The ML model approach proposed by [13] was developed to overcome these limitations. It provides a simple and flexible framework for modeling non-stationary time series without relying on stringent distributional assumptions. Building upon this, ref. [19] proposed a seasonal adjustment method based on the ML model and demonstrated that it achieved improved performance compared with X-13ARIMA, particularly in capturing structural changes and seasonal dynamics in economic time series. In this study, we further introduce the DFDL model, which enables decomposition of components without assuming a specific distribution, providing robustness against non-normality and heteroscedasticity.

Importantly, the approaches proposed in this study should be understood as flexible and practical tools that researchers and practitioners can choose for time series decomposition, rather than universal replacements for established methods. Full-scale comparative benchmarking with STS, BSTS, STL, or X-13ARIMA-SEATS is left for subsequent research due to the extensive scope of this manuscript. Nevertheless, prior studies, particularly [19], provide evidence of the ML model's effectiveness and demonstrate its advantages in relevant settings.

Taken together, these studies show that the ML approach and its extended versions are well suited for decomposing complex wholesale sales data into constrained, seasonal, and remaining components, as well as an unusually varying component containing outliers, while maintaining flexibility and robustness. They offer a complementary option among existing methods, enabling detailed investigation of structural dynamics in the wholesale sector, which is the focus of the present study.

3. Detailed Review of Our Previous Research

3.1. ML Model Approach

As a fundamental cornerstone for the present study, in this section, we offer a comprehensive review of the ML model approach proposed by [13] and its extended versions introduced by [14,19].

3.1.1. Basic Model

Consider that decompose a time series y_t into two unobserved components as follows:

$$y_t = s_t + f_t \quad (t = 1, 2, \ldots, N) \tag{1}$$

with s_t and f_t denoting the constrained and remaining components, respectively, where t represents a specific time point, and N is the sample size. The constrained component reflects long-term variation, which is expected to be highly smoothed, while the remaining component captures short-term variation, which often represents cyclical fluctuations in the time series y_t. To ensure a unique decomposition, the average of the remaining component over a given data span is assumed to be zero.

To achieve smoothness for the constrained component, a linear model of time t is introduced as follows:

$$s_t = \alpha_n + \beta_n t, \quad (t = n, n+1, \ldots, n+k-1), \tag{2}$$

where k is an integer which represents the width of the time interval $[n, n+k-1]$ for $n = 1, 2, \ldots, N-k+1$, and α_n and β_n are the coefficients. When a centered time variable within the n-th time interval is introduced as

$$z_j = t - \bar{t}_n = j - \frac{k+1}{2} \quad (j = 1, 2, \ldots, k). \tag{3}$$

In Equation (3), $\bar{t}_n = n + \frac{k-1}{2}$ represents the midpoint of the time interval. So, by substituting $t = z_j + \bar{t}$, the model in Equation (2) is rewritten as

$$s_t = \mu_n + \beta_n z_j, \quad t = n + j - 1 \quad (j = 1, 2, \ldots, k),$$

where $\mu_n = \alpha_n + \beta_n \bar{t}_n$. The model in Equation (1) is then expressed as

$$y_t = \mu_n + \beta_n z_j + f_t, \quad t = n + j - 1 \quad (j = 1, 2, \ldots, k), \tag{4}$$

or in vector form of Equation (4) as follows:

$$\boldsymbol{y}(n) = \mu_n \mathbf{1}_k + \beta_n \boldsymbol{z} + \boldsymbol{f}(n). \tag{5}$$

In Equation (5),

$$\boldsymbol{y}(n) = \begin{bmatrix} y_{n+k-1} \\ y_{n+k-2} \\ \vdots \\ y_n \end{bmatrix}, \ \boldsymbol{z} = \begin{bmatrix} z_k \\ z_{k-1} \\ \vdots \\ z_1 \end{bmatrix}, \ \boldsymbol{f}(n) = \begin{bmatrix} f_{n+k-1} \\ f_{n+k-2} \\ \vdots \\ f_n \end{bmatrix} = \begin{bmatrix} f_1^{(n)} \\ f_2^{(n)} \\ \vdots \\ f_k^{(n)} \end{bmatrix},$$

and $\mathbf{1}_k$ denotes a k-dimensional vector in which all elements are 1.

Furthermore, we set

$$\boldsymbol{f}(n-1) = (f_{n+k-2}, f_{n+k-3}, \ldots, f_{n-1})^{\mathtt{t}} = (f_1^{(n-1)}, f_2^{(n-1)}, \ldots, f_k^{(n-1)})^{\mathtt{t}}$$

denoting the vector associated with the remaining component for $\boldsymbol{y}(n-1)$ in the $n-1$-th time interval. It can be observed that $f_j^{(n)}$ and $f_{j-1}^{(n-1)}$ represent the same term, namely, f_{n+k-j}, of the remaining component for $j = 2, 3, \ldots, k$. However, they may undergo slight changes to accommodate for $\boldsymbol{y}(n-1)$ and $\boldsymbol{y}(n)$ in the $(n-1)$-th and n-th time intervals. Thus, for a given value of n, the following relationship holds:

$$f_j^{(n)} = f_{j-1}^{(n-1)} + e_{n+1-j} \quad (j = 2, 3, \ldots, k), \tag{6}$$

where e_{n+1-j} represents the variation between $f_j^{(n)}$ and $f_{j-1}^{(n-1)}$.

The model introduced above is referred to as the ML model, and the approach based on this model is called the ML model approach.

3.1.2. Estimation of Remaining Component

In Equation (6), the quantities μ_n, β_n, and $\boldsymbol{f}(n)$ are treated as the parameters. To achieve stable parameter estimates, a Bayesian approach was adopted.

First, it was assumed that μ_n and β_n exhibit smooth variations with respect to n as

$$\mu_n = \mu_{n-1} + \varepsilon_n, \quad \beta_n = \beta_{n-1} + \phi_n \tag{7}$$

under diffuse priors for ε_n and ϕ_n. That is, we assume that $\varepsilon_n \sim \mathcal{N}(0, \eta^2)$ and $\phi_n \sim \mathcal{N}(0, \eta^2)$ in Equation (7), where the variance η^2 can be set to a sufficiently large value.

Furthermore, to obtain stable estimates for the remaining component, it is assumed that $\boldsymbol{f}(n)$ is orthogonal to $\mathbf{1}_k$ and $\boldsymbol{z}$. Thus, the following equation is introduced:

$$\mathbf{1}_k^{\mathsf{t}} \boldsymbol{f}(n) \approx 0, \quad \boldsymbol{z}^{\mathsf{t}} \boldsymbol{f}(n-1) \approx 0. \tag{8}$$

Applying Equation (6) to the relations in Equation (8), we set

$$f_1^{(n)} = -\sum_{j=1}^{k-1} f_j^{(n-1)} + e_{n+k-1}, \quad f_2^{(n)} = -\sum_{j=2}^{k} \frac{z_{k-j}}{z_k} f_j^{(n-1)} + e_{n+k-2}. \tag{9}$$

Here, Equation (9) represents the priors for $f_1^{(n)}$ and $f_2^{(n)}$. Moreover, the priors for $f_j^{(n)}$ are established as follows:

$$f_j^{(n)} = f_{j-1}^{(n-1)} + e_{n+k-j} \quad (j = 3, 4, \ldots, k). \tag{10}$$

In Equation (10), $e_n, e_{n-1}, \ldots, e_{n-k+1}$ represent a set of system noises. It was assumed that $e_n \sim \mathcal{N}(0, \sigma^2)$ and $e_m \sim \mathcal{N}(0, \sigma^2)$ are independent for $m \neq n$, where σ^2 is regarded as an unknown parameter.

Furthermore, under the settings

$$\boldsymbol{x}_n = \begin{bmatrix} \mu_n \\ \beta_n \\ f_1^{(n)} \\ f_2^{(n)} \\ \vdots \\ f_k^{(n)} \end{bmatrix}, \quad \boldsymbol{F} = \begin{bmatrix} 1 & 0 & 0 & \cdots & \cdots & \cdots & \cdots & 0 \\ 0 & 1 & 0 & \cdots & \cdots & \cdots & \cdots & 0 \\ 0 & 0 & -1 & -1 & \cdots & \cdots & -1 & 0 \\ 0 & 0 & 0 & -\frac{z_{k-1}}{z_k} & -\frac{z_{k-2}}{z_k} & \cdots & \cdots & -\frac{z_1}{z_k} \\ 0 & 0 & 0 & 1 & 0 & \cdots & \cdots & 0 \\ \vdots & \vdots & \vdots & 0 & \ddots & \ddots & & \vdots \\ \vdots & \vdots & \vdots & \vdots & \ddots & \ddots & \ddots & \vdots \\ 0 & 0 & 0 & 0 & \cdots & 0 & 1 & 0 \end{bmatrix}, \tag{11}$$

$$\boldsymbol{v}_n = \begin{bmatrix} \varepsilon_n \\ \phi_n \\ e_{n+k-1} \\ e_{n+k-2} \\ \vdots \\ e_n \end{bmatrix}, \quad \boldsymbol{G} = \boldsymbol{I}_{k+2}, \quad \boldsymbol{H} = \begin{bmatrix} \mathbf{1}_k & \boldsymbol{z} & \boldsymbol{I}_k \end{bmatrix}, \tag{12}$$

with $\boldsymbol{I}_k$ denoting a k-dimensional unit matrix, a set of a Bayesian model for the ML model can be expressed by a state-space form as

$$\boldsymbol{x}_n = \boldsymbol{F}\boldsymbol{x}_{n-1} + \boldsymbol{G}\boldsymbol{v}_n, \tag{13}$$

$$\boldsymbol{y}(n) = \boldsymbol{H}\boldsymbol{x}_n \tag{14}$$

with $\boldsymbol{v}_n \sim \mathrm{N}(\mathbf{0}, \boldsymbol{Q})$, where $\boldsymbol{Q} = \mathrm{diag}(\eta^2, \eta^2, \sigma^2, \ldots, \sigma^2)$. Here, $\boldsymbol{F}$, $\boldsymbol{G}$, and $\boldsymbol{H}$ in Equations (13) and (14) are defined in Equations (11) and (12).

Thus, given the initial conditions $\boldsymbol{x}_{0|0}$ and $\boldsymbol{V}_{0|0}$, as well as the observations $Y_{1:N} = \{y_1, y_2, \ldots, y_N\}$, we can obtain the mean vectors and the covariance matrices of the state $\boldsymbol{x}_n$ for $n = 1, 2, \ldots, N-k+1$ using the following Kalman filter, which is composed of a *one-step-ahead prediction* step and a *filter* step (see, e.g., [8]):

[**One-step-ahead prediction**]:

$$\begin{aligned} \boldsymbol{x}_{n|n-1} &= \boldsymbol{F}\boldsymbol{x}_{n-1|n-1}, \\ \boldsymbol{V}_{n|n-1} &= \boldsymbol{F}\boldsymbol{V}_{n-1|n-1}\boldsymbol{F}^{\mathsf{t}} + \boldsymbol{G}\boldsymbol{Q}\boldsymbol{G}^{\mathsf{t}}. \end{aligned}$$

[**Filter**]:

$$\begin{aligned} \boldsymbol{K}_n &= \boldsymbol{V}_{n|n-1}\boldsymbol{H}^{\mathsf{t}}(\boldsymbol{H}\boldsymbol{V}_{n|n-1}\boldsymbol{H}^{\mathsf{t}})^{-1}, \\ \boldsymbol{x}_{n|n} &= \boldsymbol{x}_{n|n-1} + \boldsymbol{K}_n(\boldsymbol{y}(n) - \boldsymbol{H}\boldsymbol{x}_{n|n-1}), \\ \boldsymbol{V}_{n|n} &= (\boldsymbol{I}_{k+2} - \boldsymbol{K}_n\boldsymbol{H})\boldsymbol{V}_{n|n-1}. \end{aligned}$$

Moreover, the final estimate of $\boldsymbol{x}_n$ is obtained using the following *fixed-interval smoothing* for $n = N-k, N-k-1, \ldots, 1$.

[**Fixed-interval smoothing**]:

$$\begin{aligned} \boldsymbol{A}_n &= \boldsymbol{V}_{n|n}\boldsymbol{F}^{\mathsf{t}}\boldsymbol{V}_{n+1|n}^{-1}, \\ \boldsymbol{x}_{n|N} &= \boldsymbol{x}_{n|n} + \boldsymbol{A}_n(\boldsymbol{x}_{n+1|N} - \boldsymbol{x}_{n+1|n}), \\ \boldsymbol{V}_{n|N} &= \boldsymbol{V}_{n|n} + \boldsymbol{A}_n(\boldsymbol{V}_{n+1|N} - \boldsymbol{V}_{n+1|n})\boldsymbol{A}_n^{\mathsf{t}}. \end{aligned}$$

So, we can obtain the estimation results for the components' decomposition based on the results of the above fixed-interval smoothing. Note that the fixed-interval smoothing results for $n = N-k+1$ are contained in the results of the above Kalman filter.

Indeed, by incorporating f_t for $t = 1, 2, \ldots, N$ in the state vector $\boldsymbol{x}_n$ for $n = 1, 2, \ldots, N-k+1$, the estimate of the remaining component can be obtained through the state-space model described by Equations (13) and (14). The posterior distribution for the state vector $\boldsymbol{x}_n$, characterized by $\boldsymbol{x}_{n|N}$ and $\boldsymbol{V}_{n|N}$, follows a Gaussian distribution. Therefore, the estimate $\widehat{f}_t$ of f_t can be obtained from $\boldsymbol{x}_{n|N}$ for $n = 1, 2, \ldots, N-k+1$. Concretely, the $\widehat{f}_t$ values for $t = k, k-1, \ldots, 1$ are obtained as the corresponding third through the $(k+2)$-th elements in the vector $\boldsymbol{x}_{1|N}$, and the $\widehat{f}_t$ values for $t = k+1, k+2, \ldots, N$ are given by taking each the third element in the vector $\boldsymbol{x}_{n|N}$ for $n = 2, 3, \ldots, N-k+1$. Consequently, the estimate $\widehat{s}_t$ of the constrained component s_t is given by $\widehat{s}_t = y_t - \widehat{f}_t$.

For estimating the parameters k and σ^2, a likelihood function was constructed (for the detail, see [13]). Thus, these parameters can be estimated using the maximum likelihood method.

3.2. Extension of ML Model Approach

When handling time-series data in which abnormal fluctuations, in addition to the constrained and remaining components, are regarded as outliers, it becomes essential to concurrently decompose the time series and identify the number and locations of these outliers, isolating them from each component. To address this, ref. [14] introduced a method as an extension of the ML model approach. In this section, we will conduct a review concerning this approach. This will be applied in the first part of the empirical analysis.

3.2.1. Extended ML Model for Outlier Estimation

Consider here a case that the time series y_t contains some outliers. For estimating the outliers, the model in Equation (1) was modified as follows:

$$y_t = s_t + f_t + h_t \quad (t = 1, 2, \ldots, N), \tag{15}$$

where h_t represents the time series for the unusually varying component, which may include outliers, while the other variables and related assumptions remain consistent with the model in Equation (1). When we set $u_t = 0$ for $t = 1, 2, \ldots, N$, then the model in Equation (15) is equivalent to the ML model in Equation (1). Thus, we refer to the model in Equation (15) as the *extended ML model*.

Recalling the settings in Section 3.1, the model in Equation (15) can be expressed as follows:

$$\boldsymbol{y}(n) = \mu_n \mathbf{1}_k + \beta_n \boldsymbol{z} + \boldsymbol{f}(n) + \boldsymbol{h}(n). \tag{16}$$

In Equation (16), $\boldsymbol{h}(n) = (h_{n+k-1}, h_{n+k-2}, \ldots, h_n)^\mathsf{t}$, and the definitions for other symbols remain unchanged from those in Equation (6). Furthermore, we assume that the values for almost all elements in $\{h_1, h_t, \ldots, h_N\}$ representing the time series of the unusually varying component can be set to zero, except for possibly m non-zero parameters denoted as $\boldsymbol{\delta} = (\delta_1, \delta_2, \ldots, \delta_m)^\mathsf{t}$, expressing the potential outliers, with $m << N$ being the number.

Originally each outlier is treated as a constant parameter. However, for computational efficiency in the estimation process, they are formally considered as time-varying random variables. For instance, δ_j for $j = 1, 2, \ldots, m$ is represented as δ_{jn}, and a transition equation

$$\delta_{jn} = \delta_{j(n-1)} \quad (n = 1, 2, \ldots, N; j = 1, 2, \ldots, m) \tag{17}$$

is introduced, i.e., it remains constant over the transition with $n = 1, 2, \ldots, N - k + 1$.

By incorporating the transition equation in Equation (17) as priors for the outliers, the state vector and the related matrices are redefined as follows:

$$\boldsymbol{x}_n = \begin{bmatrix} \mu_n \\ \beta_n \\ f_1^{(n)} \\ f_2^{(n)} \\ \vdots \\ f_k^{(n)} \\ \delta_{1n} \\ \delta_{2n} \\ \vdots \\ \delta_{mn} \end{bmatrix}, \quad \boldsymbol{F} = \begin{bmatrix} 1 & 0 & 0 & \cdots & \cdots & \cdots & \cdots & 0 & \\ 0 & 1 & 0 & \cdots & \cdots & \cdots & \cdots & 0 & \\ 0 & 0 & -1 & -1 & \cdots & \cdots & -1 & 0 & \\ 0 & 0 & 0 & -\frac{z_{k-1}}{z_k} & -\frac{z_{k-2}}{z_k} & \cdots & \cdots & -\frac{z_1}{z_k} & \boldsymbol{O} \\ 0 & 0 & 0 & 1 & 0 & \cdots & \cdots & 0 & \\ \vdots & \vdots & \vdots & 0 & \ddots & \ddots & & \vdots & \\ \vdots & \vdots & \vdots & \vdots & \ddots & \ddots & \ddots & \vdots & \\ 0 & 0 & 0 & 0 & \cdots & 0 & 1 & 0 & \\ & & & & \boldsymbol{O} & & & & \boldsymbol{I}_m \end{bmatrix},$$

$$\boldsymbol{G} = \begin{bmatrix} \boldsymbol{I}_{k+2} \\ \boldsymbol{O} \end{bmatrix}, \quad \boldsymbol{H}_n = \begin{bmatrix} & & & \psi_{n+k-1} & & & & \\ & & & & \psi_{n+k-2} & & & \\ \mathbf{1}_k & \boldsymbol{z} & \boldsymbol{I}_k & & & \ddots & & \\ & & & & & & \ddots & \\ & & & & & & & \psi_n \end{bmatrix},$$

where $\boldsymbol{I}_m$ denotes an m-dimensional identity matrix, $\boldsymbol{O}$ represents a zero matrix with appropriate numbers of rows and columns, and ψ_i denotes a concatenation function with the definition that if $h_i = \delta_j$, then $\psi_i = 1$ and $\psi_i = 0$; otherwise, for $i = n + k - 1, n + k - 2, \ldots, n$ and $j = 1, 2, \ldots, m$.

Then, based on the aforementioned adjustments and employing $\boldsymbol{H} = \boldsymbol{H}_n$, the state-space expression for the expanded ML model can be expressed in the equations in Equations (13) and (14). Consequently, the estimate $\widehat{\boldsymbol{\delta}}$ for the outliers, along with those for the remaining component, can be obtained from $\boldsymbol{x}_{n|N}$ for $n = 1, 2, \ldots, N - k + 1$. Specif-

ically, $\widehat{\boldsymbol{\delta}}$ is determined as the elements ranging from the $(k+3)$-th to the $(k+2+m)$-th positions in the vector $\boldsymbol{x}_{N-k+1|N}$, which solely relies on the filter results at $n = N-k+1$.

3.2.2. Estimating the Locations and Number of Outliers

When k is given, most of the outliers become assimilated into the estimate of the remaining component. Let $\widetilde{f}_t$ denote the initial estimates for the remaining component for $t = 1, 2, \ldots, N$ using the ML model approach. Then, a rule for determining the locations of outliers can be constructed as follows.

It is assumed that a large $\widetilde{f}_t^2$ may likely contain δ_t^2. Thus, if $\widetilde{f}_{t_1}^2 \geq \widetilde{f}_{t_2}^2 \geq \cdots \geq \widetilde{f}_{t_N}^2$, it is reasonable to infer that $\widetilde{f}_{t_1}$ contains the largest outlier, $\widetilde{f}_{t_2}$ contains the second largest outlier, and so forth. Put differently, when considering the number of outliers as m, one can establish the order in which to search for potential outlier locations as $t_1, t_2, \ldots, t_m$. Subsequently, the locations of outliers can be determined based on this order.

Furthermore, when specifying the outliers $\boldsymbol{\delta} = (\delta_{t_1}, \delta_{t_2}, \ldots, \delta_{t_m})^{\mathsf{t}}$ with specific locations and the number m of the outliers, the time series h_t for the unusually varying component becomes a function of these outliers. Consequently, the outlier-adjusted time series $z_t = y_t - h_t$ also becomes a function of $\boldsymbol{\delta}$. So, the log-likelihood for the outliers, together with other parameters such as k and σ^2, can be constructed.

Thus, a maximum likelihood method was applied to estimate these parameters containing outliers. As a function of m, the Akaike information criterion (AIC) can then be defined, and the optimal value of m is determined using the minimum AIC method [20]. More recently, approaches for detecting and estimating outliers have been further refined in both theoretical and methodological aspects [21].

3.2.3. Extension for Time Series with Seasonality

In [19], the ML model approach was applied to time-series data containing a seasonal component. The key to resolving this issue lies in estimating the seasonal component. Once the seasonal component is estimated, we can remove it from the time series, resulting in a seasonally adjusted time series. Subsequently, the aforementioned extended ML model approach can be employed to address anomalies in the seasonally adjusted time series (see [14]).

4. First Illustrative Example

In this example, we provide an empirical analysis of the dynamics in the structure of wholesale sales in Japan. As outlined in the introduction, the main aim of this study is to analyze the structural changes in Japan's wholesale sales value. However, the original data are complex in structure, making it challenging to directly discern their structural features. Therefore, we initially utilized the extended ML model approach to decompose it into components. Subsequently, for each decomposed component, we analyzed the temporal variations from a socio-economic perspective. Furthermore, the results of decomposition also served as preparatory work for the subsequent second illustrative example.

4.1. Data and Objectives

As mentioned in the introduction, this study focuses on wholesale sales in Japan, leveraging the comprehensive and well-defined nature of their data. With wholesale sales categorized into 12 distinct business types, this research seeks to conduct a thorough analysis, delving into the structural changes within each type and investigating the effects of business fluctuations. The significance of wholesale sales extends beyond economic metrics, providing insights into global trends, societal shifts, and the ramifications of unexpected events such as economic downturns or natural disasters. Specifically, we will

examine the influences stemming from the serious financial shock around the world of 2008–2009 and the COVID-19 pandemic. The severe financial shock that occured around the world in 2008–2009 has been commonly termed as the global financial crisis, which led the subsequent stagnation and slow recovery in the world economy. As is also well known, the COVID-19 pandemic broke out in Wuhan, Hubei Province, China, in December 2019 and spread to almost every country in the world in March 2020, resulting in a global economic slowdown, as also took place during the global financial crisis.

Table 1 presents a list of the business types involved in wholesale sales in Japan.

Table 1. Business types of wholesale sales in Japan.

Symbol	Name
W1	General Merchandise
W2	Textiles
W3	Apparel and Accessories
W4	Livestock and Aquatic Products
W5	Food and Beverages
W6	Building Materials
W7	Chemicals
W8	Minerals and Metals
W9	Machinery and Equipment
W10	Furniture and House Furnishings
W11	Medicines and Toiletries
W12	Others

We analyzed the data for wholesale sales (WS) across the 12 business types listed in Table 1. The original data are available from Japan's Ministry of Economy, Trade, and Industry (https://www.meti.go.jp/english/statistics/index.html, accessed on 1 May 2023). Each business type's data form a monthly time series spanning from January 1980 to December 2022, totaling $N = 516$ months, with the data measured in units of one billion JPY. To facilitate analysis, we applied a logarithmic transformation to each type's time series, resulting in logarithmically transformed WS, denoted as log-WS. The log-WS data for each business type constitute the objective of our analysis. Figure 1 shows graphs of log-WS time series from W1 to W6 in Japan (January 1980 to December 2022).

Figure 2 depicts graphs of log-WS time series from W7 to W12 in Japan (January 1980 to December 2022).

In both sets of time series plots for log-WS from W1 to W6 (Figure 1) and from W7 to W12 (Figure 2), we observe two prominent abrupt fluctuations. The first occurred around early 2009, indicating a sharp decline in levels attributed to the global financial crisis. The second abrupt change occurred around early 2020, which was marked by a sharp shift in levels. This is likely a consequence of the shock induced by the rapid spread of the COVID-19 pandemic. Interestingly, during the second abrupt change, there is a more noticeable increase in levels than a decrease. Additionally, the time series exhibit significant seasonal variations. Our main goal in analyzing the time series data of log-WS was to gain insights into the dynamic structure of wholesale sales in Japan. To achieve this, we first decomposed each time series into four components, i.e., the constrained, remaining, seasonal, and unusually varying components. Next, we delved into the characteristics of

variations within each component, aiming to understand the factors driving the observed structural changes in each component.

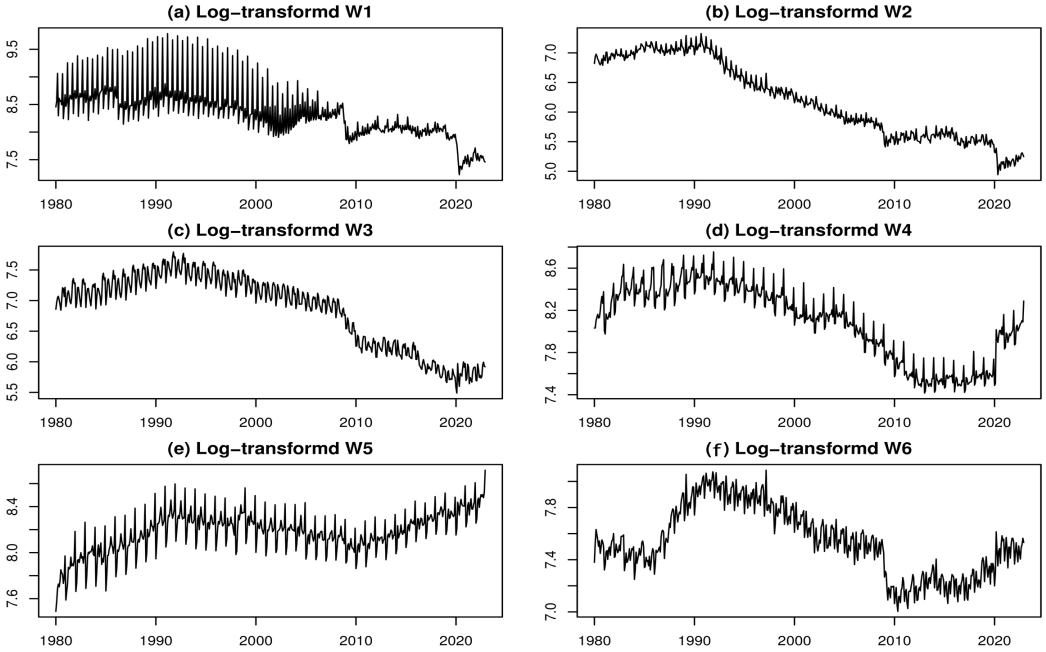

Figure 1. log-WS time series from W1 to W6 in Japan (January 1980 to December 2022).

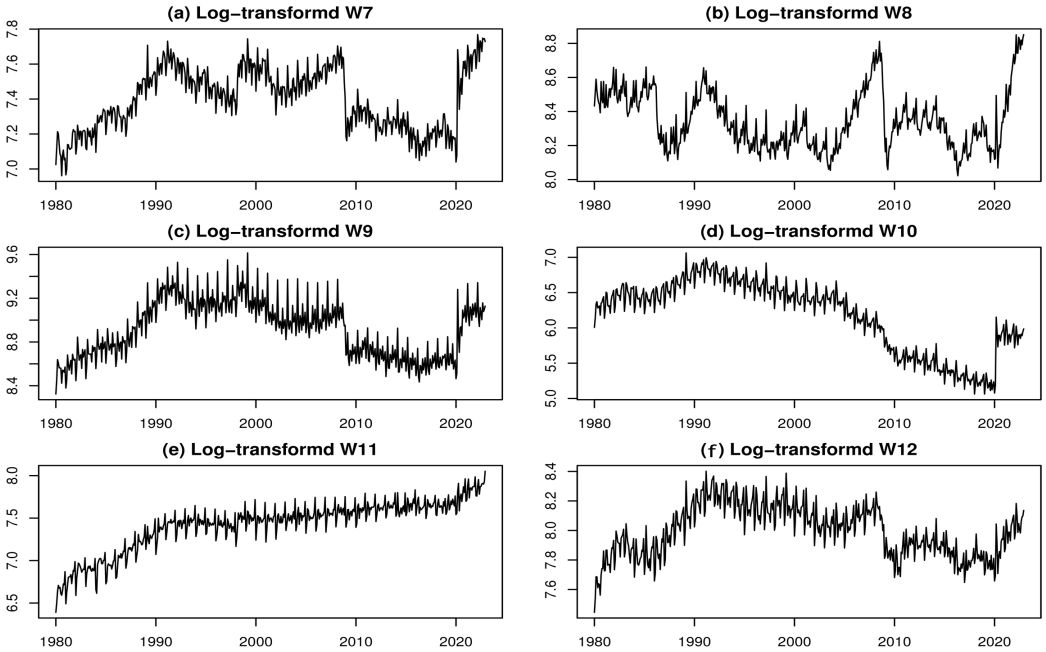

Figure 2. log-WS time series from W7 to W12 in Japan (January 1980 to December 2022).

4.2. Analyzing Time-Series Data for General Merchandise (W1)

In this subsection, we delve into the log-WS time-series data for the general merchandise (W1), providing a detailed walkthrough of the analytical process to illustrate the methodology effectively.

To initiate the analysis, we began by performing seasonal adjustment on the time series. Initially, the monthly time-series data were divided into 12 annual time-series units, each comprising data for the corresponding month. Each annual time-series data sample underwent decomposition into a composite component, which includes both constrained and seasonal components, as well as a remaining component containing outliers, utilizing

the ML model approach. This decomposition process was executed for each value of k (which denotes the width of the time interval for the first-time decomposition) within the range of 3 to 35. Utilizing the average of log-likelihood computation, we pinpointed the maximum value at $k = 31$, denoted as $\widehat{k}_1$. Subsequently, the decomposition was conducted using $\widehat{k}_1 = 31$ for each annual time series.

Next, the estimated time-series data of each composite component were sequentially synthesized into monthly time-series data. Following that, we conducted constrained and seasonal components decomposition of the monthly time series for the decomposed composite component. This involved decomposing the monthly time series of the decomposed composite component into a constrained component and a remaining component, which is equivalent to the seasonal component, using the ML model approach. Among the results obtained for k (representing the width of the time interval for the second-time decomposition) at values of $12, 2 \times 12, \ldots, 20 \times 12$, the maximum log-likelihood was achieved at $k = 12 \times 12 = 144$. This estimated value of k, denoted as $\widehat{k}_2$, informed the decomposition of the constrained and remaining components of the time series, which was conducted using $\widehat{k}_2 = 144$. The result for the remaining component was then utilized as the final estimate of the seasonal component. Furthermore, by subtracting this estimate from the original time-series data, the seasonally adjusted monthly time series was derived.

Figure 3 depicts graphs of seasonal component and seasonally adjusted data for the log-transformed time series of General Merchandise (W1).

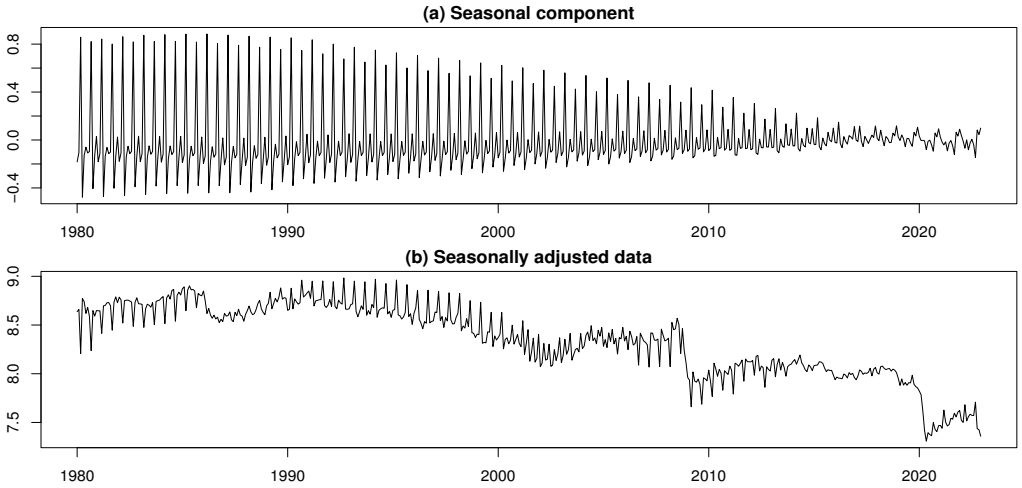

Figure 3. Seasonally adjusted results for log-transformed time series of W1.

When we observe Figure 3a, we find the following features. The estimate of the seasonal component highlights a clear seasonal pattern. However, note that the amplitude of seasonal fluctuations gradually decreases over time. More specifically, there was initially a clear seasonal variation, where the amplitude of seasonal component peaked in the early 1990s. In subsequent periods, the amplitude continued to decline. In other words, a structural change is considered to have occurred before and after the period of the early 1990s. The period from around 1992 to around 2012 is often referred to as the lost two decades of the Japanese economy (see, e.g., [22]). That is, clear structural changes can be confirmed in the sector of general merchandise during the lost two decades of the Japanese economy. This observation suggests a potential shift in consumer behavior or economic conditions influencing seasonal sales patterns in the sector of general merchandise. Such insights into the seasonal dynamics of General Merchandise can inform strategic decision-making behavior and resource allocation for businesses operating in this sector. Moreover, looking at the graph of seasonally adjusted data in Figure 3b, we notice that the pattern of seasonally adjusted values changed abruptly in the late 2000s and early 2020s. These

two pattern changes can be attributed to the following events. The sharp decline in seasonally adjusted data at the end of the 2000s is closely related to the global financial crisis. In addition, the sharp decline in seasonally adjusted values in the early 2020s can be regarded as attributable to the COVID-19 pandemic.

Furthermore, our extended ML model approach was applied to the seasonally adjusted time series. In this step, to execute the extended ML approach, we needed to estimate the value of k (which denotes the width of the time interval for the third-time decomposition). The results indicate that the estimated value of k, denoted as $\widehat{k}_3$, is 63, and the number of outliers is estimated to be $\widehat{m} = 3$. Based on the magnitude of their amplitude, the outliers are estimated to occur at time points 351, 485, and 3, according to the rule for identifying outlier locations. These correspond to March 2009, May 2020, and March 1980, respectively. Figure 4 shows the final decomposition results.

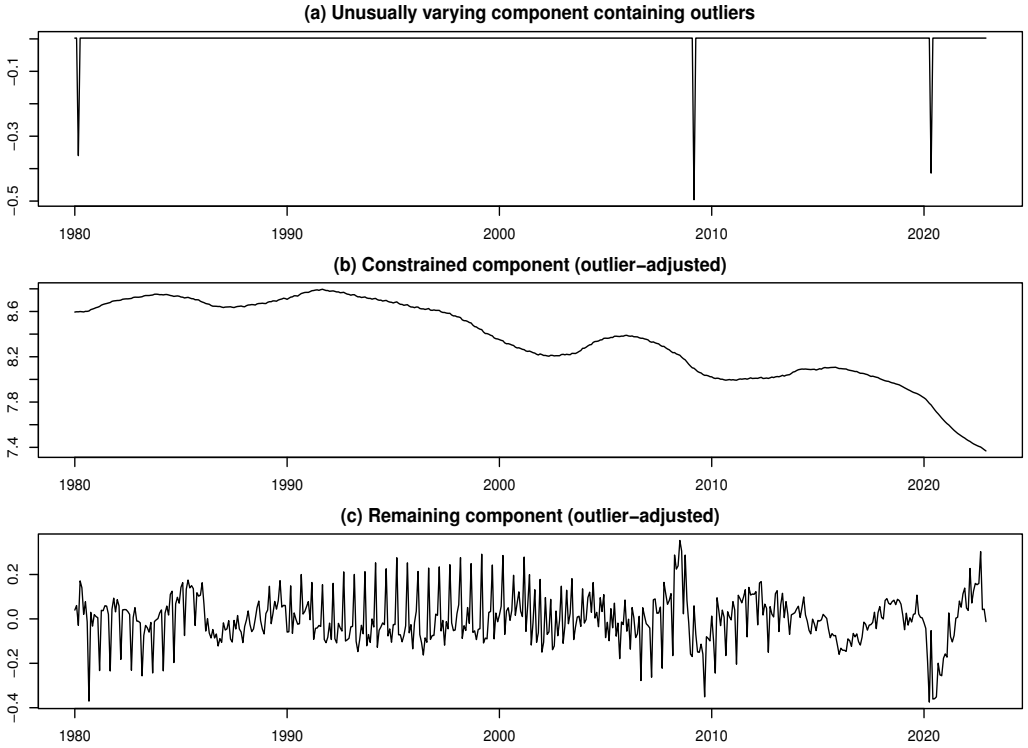

Figure 4. Decomposed results for log-transformed time series of W1.

Figure 4a illustrates the estimate for the unusually varying component, containing outliers. Figure 4b,c present the estimates for the constrained component (representing the trend) and the remaining component (representing cyclical variations), respectively. The following can be seen from each panel of Figure 4. From panel (a), three negative outliers stand out at first glance. These outliers suggest that business fluctuations were influenced by unforeseen events or external shocks. We observe that the shape of the graph of the constrained component in panel (b) changes (i.e., there are changes in the trend) around the time when these significant negative outliers are observed. The significant negative outliers in the late 2000s and early 2020s are considered to be closely related to the global financial crisis and the COVID-19 pandemic, respectively, as described above. The significant negative outlier in the early 1980s may be related to the second oil crisis of 1979–1980. In the graph of the residual component in panel (c), we also observe significant fluctuations with large amplitudes in the early 1980s, late 2000s, and early 2000s. Based on the above results, several key insights can be derived from an economic perspective. The downturn between 2008 and 2009 appears to be a consequence of the global financial crisis. This widespread financial market turmoil led to a decline in corporate and consumer

confidence, contributing to a sharp economic contraction. The downturn in the beginning of 2020 can be attributed to the COVID-19 pandemic. Global containment measures restricted business operations and international trade, directly impacting economic activities. In other words, demand for wholesale products of general merchandise decreased during the global financial crisis and the COVID-19 pandemic.

A comprehensive examination of the graphs in Figures 3 and 4 yields important policy implications. Specifically, it is essential to accumulate findings based on theoretical and empirical studies of effective economic stabilization policies against enormous shocks such as the global financial crisis and the COVID-19 pandemic. The results from our analysis also suggest the need to construct an institutional design that allows for the implementation of appropriately timed policies that take advantage of rigorous economic theory and evidence-based macroeconomic policy findings to respond to the exogenous shocks described above when they occur.

4.3. Analyzing Time-Series Data for Textiles (W2)

In this section, we present the estimates of the time-series data for log-WS in the second type, namely, Textiles (W2). Starting from this section, we proceed with decomposition results and conducting analysis for each type of WS. The estimation process mirrors that of General Merchandise (W1), and consequently, we omit its repetition. The ensuing discussion solely encompasses the results and economic analysis. Figure 5 depicts graphs of seasonal component and seasonally adjusted data for the log-transformed time series of Textiles (W2).

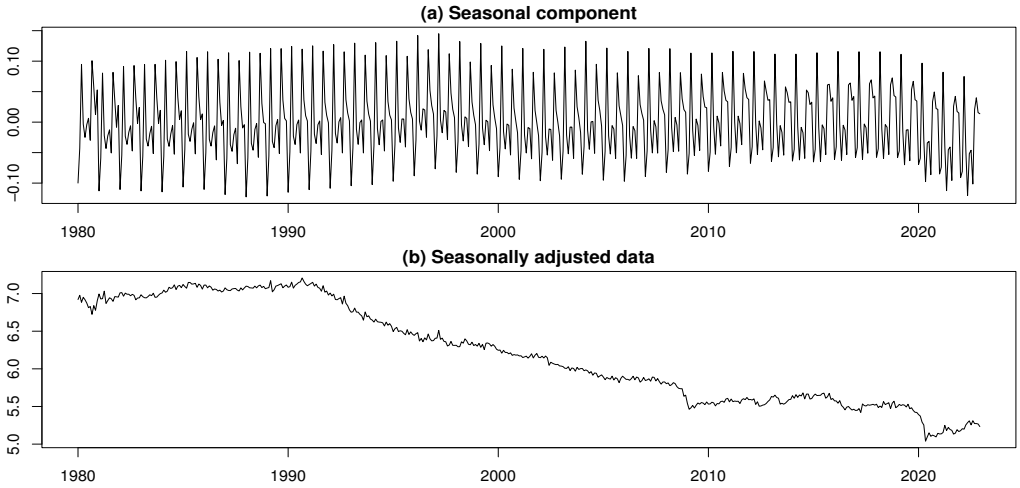

Figure 5. Seasonally adjusted results for log-transformed time series of W2.

The results for parameter estimation are as follows: $\widehat{k}_1 = 25$, $\widehat{k}_2 = 96$, $\widehat{k}_3 = 76$, and $\widehat{m} = 21$. The first 10 outliers are estimated at time points 485, 486, 488, 490, 489, 491, 9, 350, 492, and 487. While these outliers span a wide range, with notable ones are still observed in the early part of 2009 and mid-2020. This aligns with the results observed in the analysis of W1 and does not deviate significantly.

Compared to Figure 3a, Figure 5a shows consistently large amplitudes throughout the analysis period. Although the general shapes of the trends in Figures 3b and 5b are similar, the graph in Figure 5 appears relatively smoother. Similar to Figure 3b, Figure 5b also shows a sharp decline in wholesale textile sales during the respective periods of the global financial crisis and the COVID-19 pandemic. However, Figure 5b shows a consistent decline in wholesale textile demand since the 1990s. However, unlike the graph in Figure 3b, the graph in Figure 5b is characterized by a consistent decline in wholesale textile sales since the 1990s. Ref. [22] described that in the early 1990s, the bubble burst, which then

caused a profound and prolonged shock to the Japanese economy. In other words, it can be seen that the Japanese textile wholesale industry was greatly affected by the negative impact of the bursting of Japan's bubble economy.

The final decomposition results are presented in Figure 6.

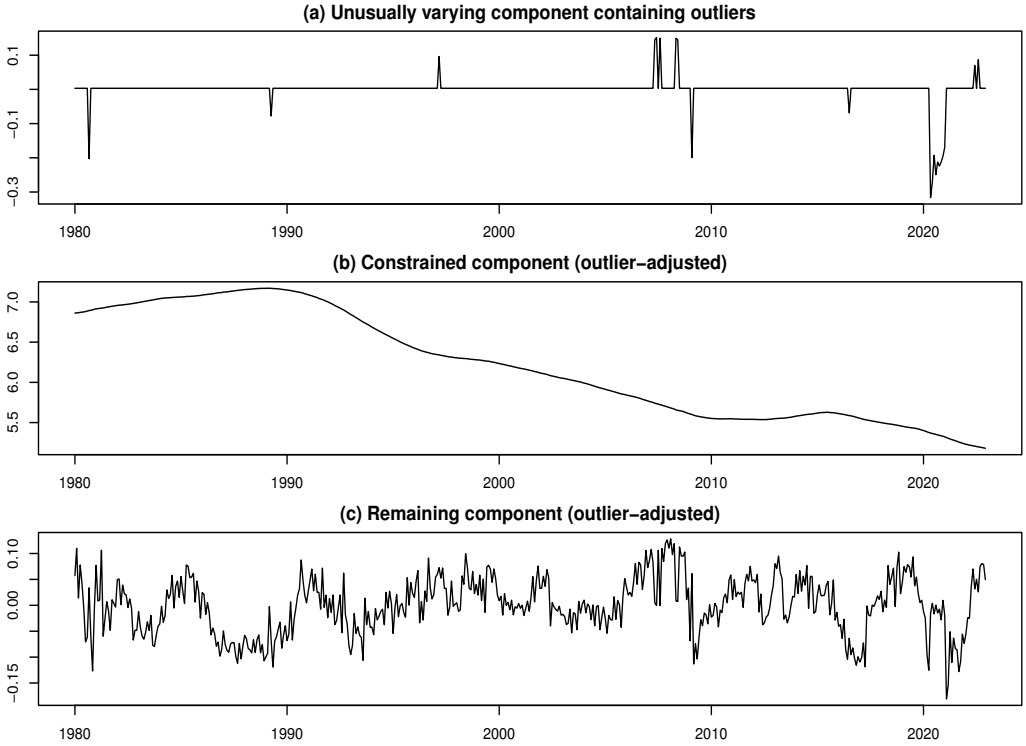

Figure 6. Decomposed results for log-transformed time series of W2.

It is noteworthy that the graph in Figure 6b shows a characteristic shape, indicating a consistent decline in the wholesale value of textile products since the early 1990s, when Japan's bubble economy collapsed. In other words, we can confirm a clear difference in the trend of wholesale textile sales in the period before and after the collapse of Japan's bubble economy in the early 1990s. This is clear evidence that structural changes occurred in the textile sector in the early 1990s. The graph of the remaining component in Figure 6c displays the behavior of the short-term cyclical fluctuations of W2. The amplitude of the remaining component obtained from W2 is smaller than that of W1, and its cyclicality is weaker. Consequently, numerous outliers have been detected in Figure 6a.

The decomposed results for Textiles (W2) reveal structural characteristics that warrant economic consideration. The relatively large amplitude feature of the seasonal component of W2 throughout the period under analysis suggests that the textile wholesale sales market is unstable. Moreover, the weak periodicity in the remaining component of W2 implies that the cyclical pattern of textile wholesale sales is less clear, perhaps influenced by industry-specific factors such as changes in consumer preferences and production methods. Furthermore, the presence of numerous outliers in W2 may highlight the nature of the textile wholesale sales market's susceptibility to various shocks, large and small. In any case, a deeper look into the background of these outliers is needed to understand the characteristics of the wholesale textile sales market.

4.4. Analyzing Time-Series Data for Apparel and Accessories (W3)

The parameter estimation results for the time-series data of log-WS for the Apparel and Accessories (W3) are as follows: $\widehat{k}_1 = 11$, $\widehat{k}_2 = 96$, $\widehat{k}_3 = 72$, and $\widehat{m} = 28$. The first

10 outliers are estimated at time points 365, 368, 366, 341, 340, 482, 444, 338, 434, and 343. Although numerous outliers have been detected, only a few are particularly prominent.

The results of seasonal adjustment are depicted in Figure 7.

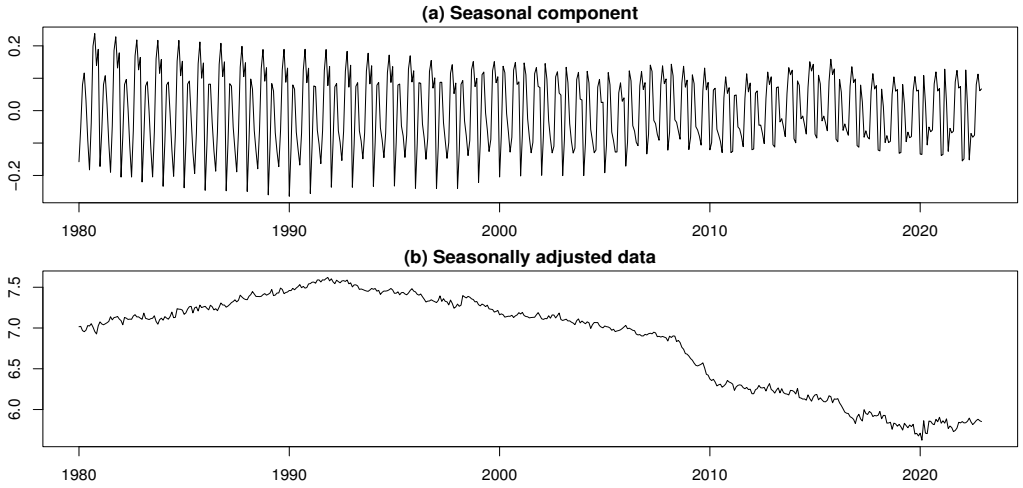

Figure 7. Seasonally adjusted results for log-transformed time series of W3.

The final decomposition results are illustrated in Figure 8.

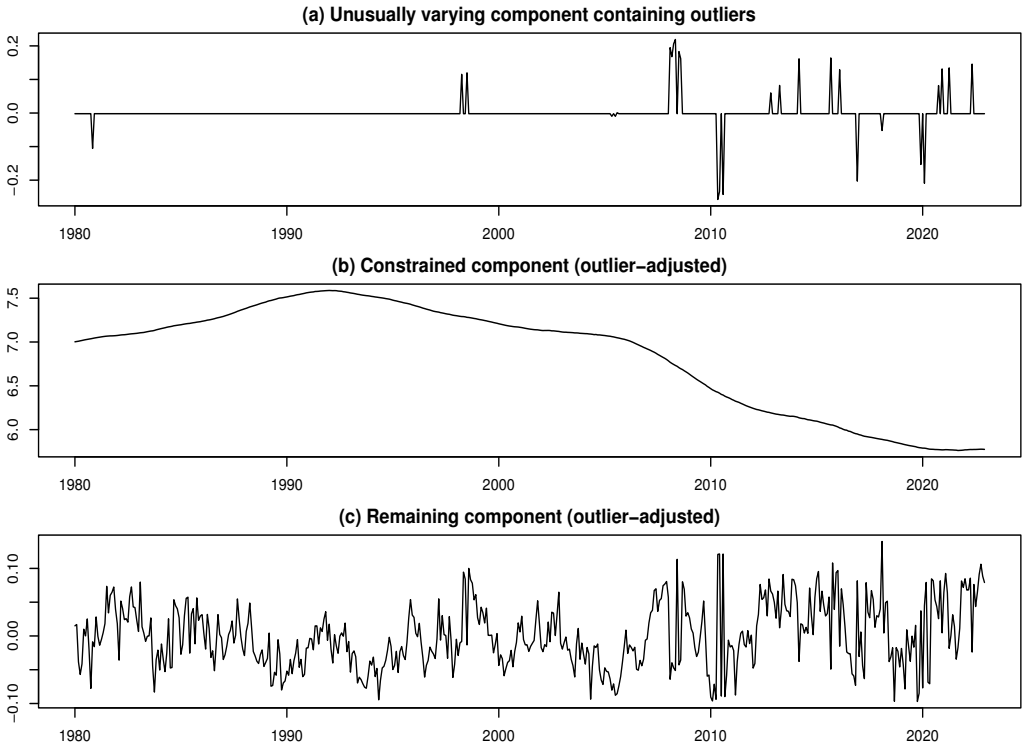

Figure 8. Decomposed results for log-transformed time series of W3.

The results for Apparel and Accessories (W3) are relatively similar to those for Textiles (W2), although the amplitude of the seasonal component, especially after the 2000s, is smaller than in the W2 case.

The estimates for W3 reveal intriguing structural patterns from an economic perspective. Observing the graph in Figure 7a, especially after the 2000s, the amplitude of seasonal fluctuations is larger in the W3 case than in the W1 case. This may indicate an inherent feature of the apparel industry that is influenced by seasonal trends and consumer preferences. The graph in Figure 7b is similar to the graph in Figure 6b in terms of the seasonally

adjusted data. Specifically, W3 shows very small fluctuations and declines during the period after the collapse of Japan's bubble economy in the early 1990s.

The numerous outliers detected in W3, as shown in Figure 8a, suggest that there is a degree of volatility or unexpected events regarding this type of wholesale sales. Figure 8b indicates that wholesale sales of apparel and accessories have been on a declining trend since the collapse of Japan's bubble economy in the early 1990s, with a further decline after the global financial crisis worsened with the collapse of Lehman Brothers in September 2008. The consistent patterns observed in the decomposition results across W2 and W3, despite slight variations, may point to industry-wide factors influencing both categories. The similarities could be attributed to shared economic conditions, market trends, or supply chain affecting both textiles and apparel and accessories types. In conclusion, we have identified the presence of structural change in the wholesale sales sector of the apparel and accessories as well. Further investigation into the unique characteristics of wholesale sales of apparel and accessories would provide additional insight into the characteristics of this market.

4.5. Analyzing Time-Series Data for Livestock and Aquatic Products (W4)

The main results for parameter estimation for Livestock and Aquatic Products (W4) are as follows: $\widehat{k}_1 = 9$, $\widehat{k}_2 = 48$, $\widehat{k}_3 = 51$, and the estimated number of outliers is $\widehat{m} = 1$. The outlier is estimated at time point 483, corresponding to March 2020, suggesting that the impact of COVID-19 on W4 was significant.

The outcomes of seasonal adjustment and the final decomposition results for Livestock and Aquatic Products (W4) are depicted in Figures 9 and 10, respectively.

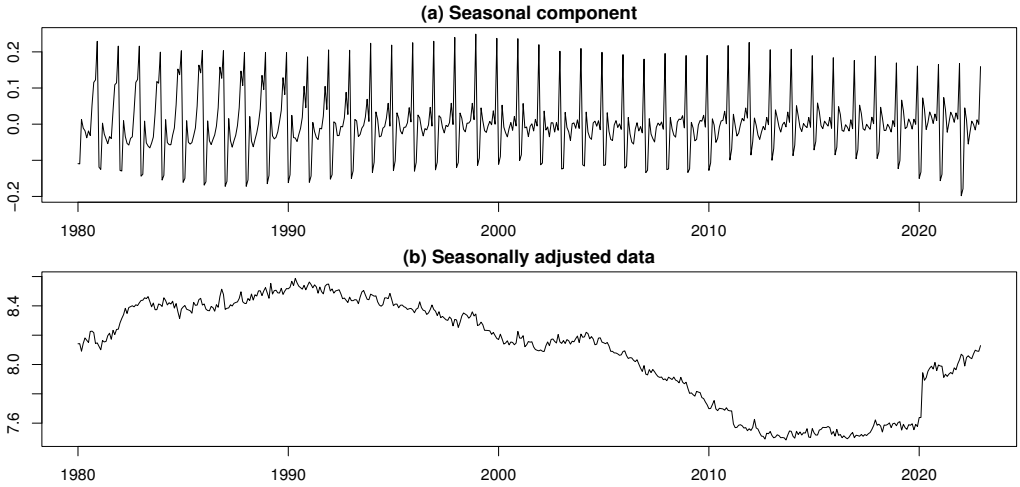

Figure 9. Seasonally adjusted results for log-transformed time series of W4.

From Figure 9a, the amplitude of seasonal variations appears generally stable, although a shift in the pattern of these fluctuations has been identified since the late 1990s. The graph of seasonally adjusted data in Figure 9b shows two striking features. First, the seasonally adjusted values of livestock and aquatic products have been declining with small fluctuations, triggered by the bubble collapse in the Japanese economy in the early 1990s. This behavior of seasonally adjusted values is similar to the case in Figure 5b for Textiles (W2) and Figure 7b for Apparel and Accessories (W3). Second, the seasonally adjusted values for livestock and aquatic products show a sharp increase in the early 2020s. This corresponds to the epidemic period of COVID-19 and can be interpreted as reflecting the increase in so-called home cooking, as the restaurant industry was forced to close.

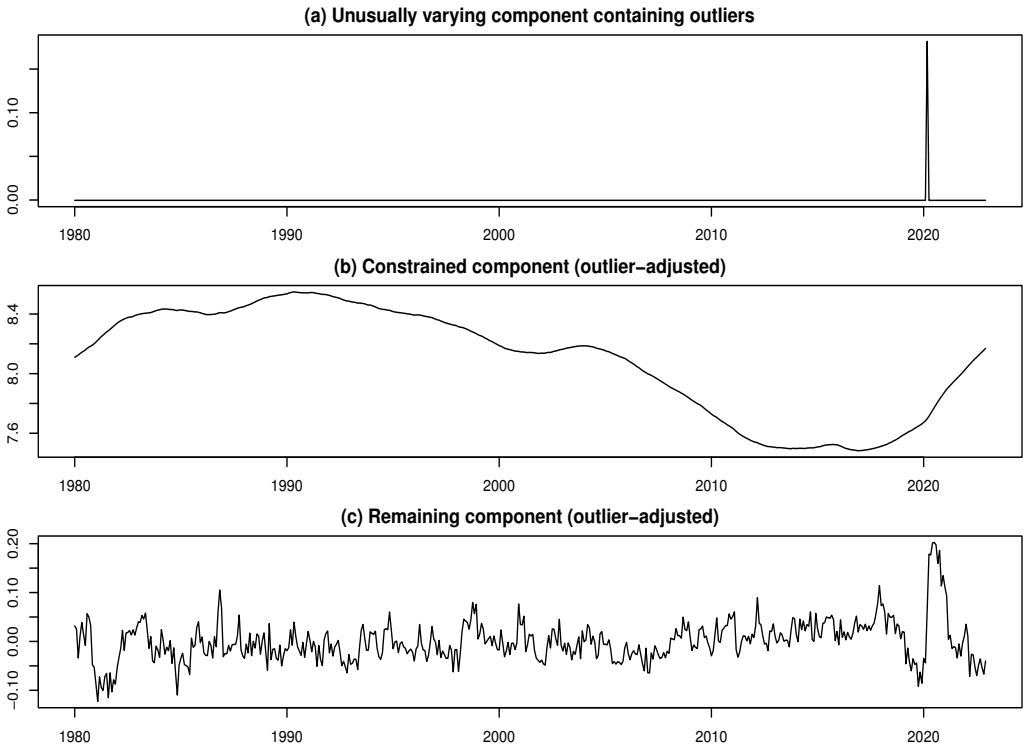

Figure 10. Decomposed results for log-transformed time series of W4.

As noted above, from the graph of unusually varying component in Figure 10a, we can identify a prominent outlier during the COVID-19 pandemic in the early 2020s. Looking at Figure 10b, the constrained component of W4 almost declined from the early 1990s to the end of the 2010s, suggesting that the food service industry may have developed rapidly during this period. However, since the early 2020s, the constrained component has been rising sharply. This trend change can be attributed to the fact that the demand for livestock and aquatic products for eating at home has increased significantly due to the COVID-19 pandemic, as mentioned above. As a result, there was a notable uptick in individuals obtaining agricultural and fishery products through distribution channels. The abrupt surge in wholesale transactions within this type can be further investigated by consulting the [23] survey report. Moreover, observing the behavior of the remaining component in Figure 10c, we can see that the amplitude is generally smaller than in the W1, W2, and W3 cases. However, we notice the presence of a large amplitude in the early 2020s. This variation clearly reflects the impact of the COVID-19 pandemic during that period.

Our analytical results can be summarized as follows. First, the discerned shift in the pattern of seasonal fluctuations since the late 1990s suggests potential structural changes in the economy or shifts in consumer behavior. A thorough understanding of these seasonal variations is essential for accurate demand forecasting and efficient resource allocation. Additionally, the sharp rise in trends for livestock and aquatic products in the early 2020s can be attributed to the impact of the COVID-19 pandemic. Notably, the closure of restaurants resulted in an upsurge in home cooking, leading to a significant spike in the procurement of agricultural and fishery products through distribution channels. This phenomenon highlights profound changes in supply chains and consumer behavior induced by the pandemic. The [23] survey report concerning the sudden surge in wholesale transactions emphasizes the importance of comprehending the specific factors and trends driving such rapid fluctuations. This information holds immense value for economists and policymakers as they contemplate future measures and policies. That is, these results are of substantial significance from an economic perspective, offering valuable insights into the factors and

repercussions of economic fluctuations. Understanding these dynamic structures is pivotal for formulating strategies aimed at fostering a sustainable economy.

4.6. Analyzing Time-Series Data for Food and Beverages (W5)

In this subsection, we examine the time-series data of log-WS for Food and Beverages (W5). The results of parameter estimation are as follows: $\widehat{k}_1 = 12$, $\widehat{k}_2 = 96$, $\widehat{k}_3 = 44$, and the estimated number of outliers is $\widehat{m} = 8$. The identified outlier locations correspond to the time points 12, 56, 226, 215, 61, 15, 218, and 216.

Figure 11 depicts graphs of seasonal component and seasonally adjusted data for the log-transformed time series of Food and Beverages (W5).

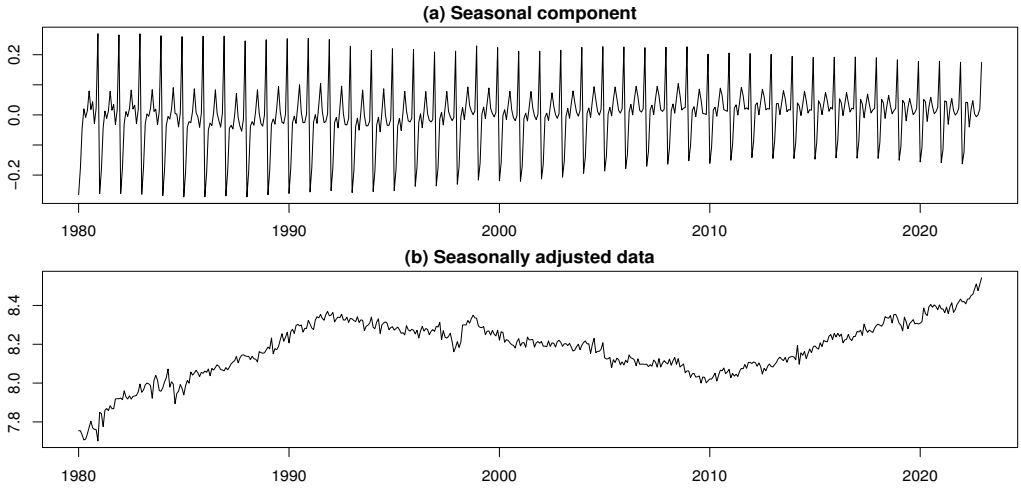

Figure 11. Seasonally adjusted results for log-transformed time series of W5.

Figure 11a shows that the fundamental pattern of the seasonal component of W5 remained relatively unchanged throughout the analyzed period. The results of the seasonal adjustment are presented in Figure 11b. The results of the seasonal adjustment process, showcased in Figure 11b, underscore the effort to eliminate seasonal variations from the data. Additionally, Figure 11b illustrates a gradual decrease in the seasonally adjusted graph during the 2000s. This may reflect the effects of bovine spongiform encephalopathy, hog cholera, and avian influenza. Ref. [24] investigated the interdependence among changes in the prices of beef, pork, and chicken in Japan using a time-varying coefficient vector autoregressive model. Their empirical analysis using monthly data from January 1990 to March 2014 showed that changes in beef prices had long-term influences on changes in pork and chicken prices. Understanding these adjustments is pivotal for accurately gauging underlying economic trends.

The final decomposition results are illustrated in Figure 12.

From Figure 12a, we find that there are numerous outliers detected in W5, suggesting a degree of volatility or unexpected events regarding the wholesale sales of W5. When we focus on Figures 11b and 12b, we can see that wholesale sales of food and beverages have further increased since 2020. This can be interpreted as a result of households having significantly more opportunities to eat at home during the coronavirus pandemic. Next, we focus on the graph of the remaining component of W5 in Figure 2c. It shows a stable pattern of short-term variations, i.e., cyclical fluctuations in the short term. The behavior of the remaining component for wholesale sales of Food and Beverages (W5) over time is similar to the case of General Merchandise (W1), with a stable pattern of fluctuations and repeated amplitudes over relatively short time intervals. The reason why the cyclical pattern of wholesale sales of food and beverages is stable can be attributed to the fact that they are daily necessities.

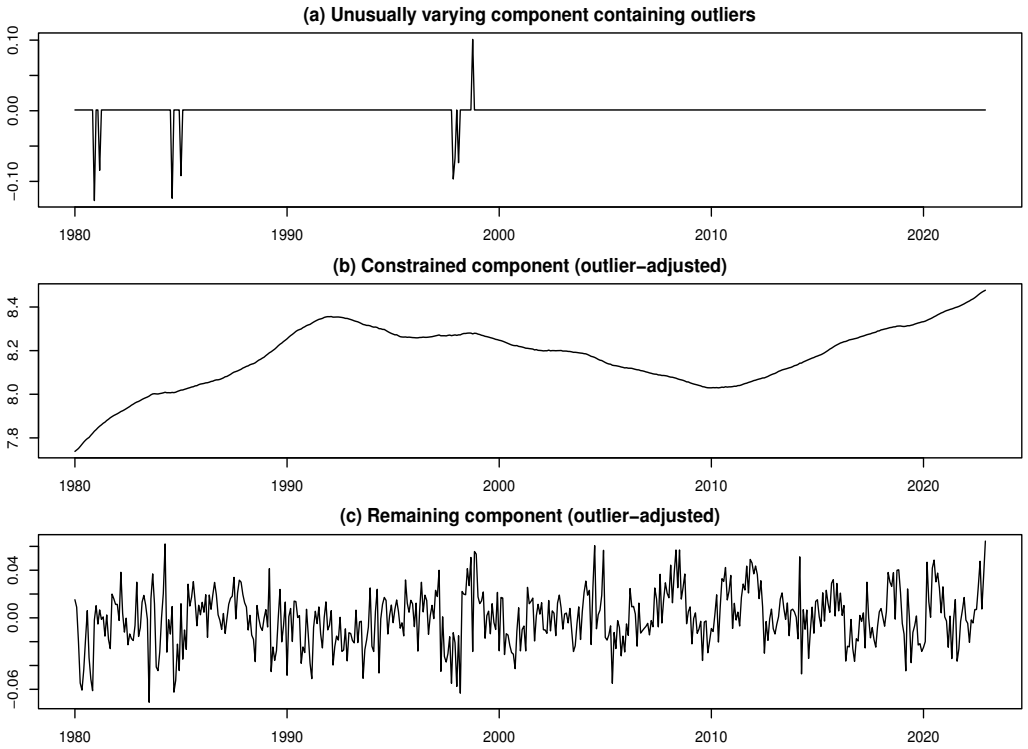

Figure 12. Decomposed results for log-transformed time series of W5.

4.7. Analyzing Time-Series Data for Building Materials (W6)

In this section, we analyze the time-series data for log-WS related to Building Materials (W6). The estimated parameters are as follows: $\widehat{k}_1 = 12, \widehat{k}_2 = 96, \widehat{k}_3 = 67$, and the estimated number of outliers is $\widehat{m} = 23$. Although numerous outliers were detected, none are considered significant.

Figure 13 shows graphs of seasonal component and seasonally adjusted data for the log-transformed time series of Building Materials (W6).

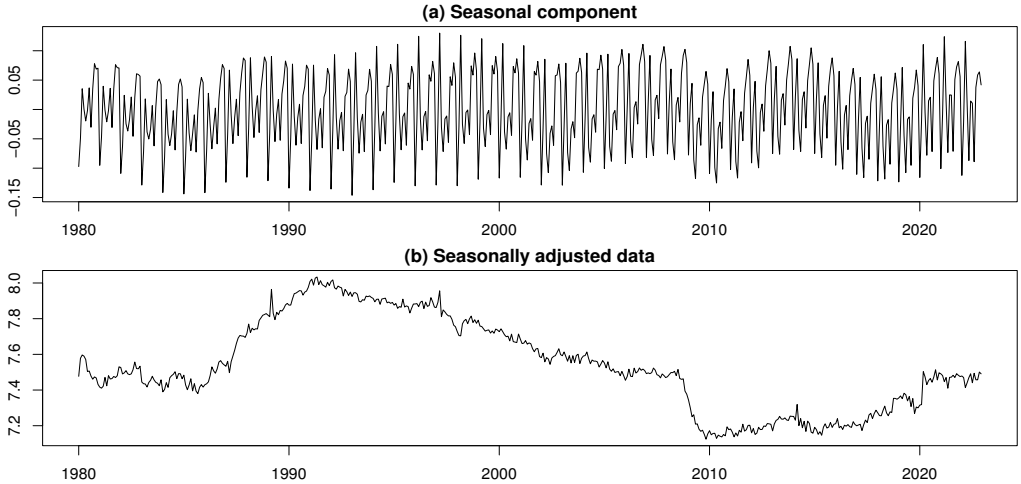

Figure 13. Seasonally adjusted results for log-transformed time series of W6.

Looking at the graphs in panels in Figure 13, we observe differences in the behavior of W6 in the period from the early 1980s to the late 1990s, from the early 1990s to the late 2000s, from the early 2010s to the late 2010s, and in the period after the 2020s. The graphs show differences in the behavior of wholesale sales of W6 in the periods from the early 1980s to the late 1990s, from the early 1990s to the late 2000s, from the early 2010s to the

late 2010s, and after the 2020s. This observation implies that the structure of the wholesale sales sector of building materials has changed throughout these periods. Thus, we obtain evidence for the existence of a dynamic structure in this sector.

The final decomposition results are illustrated in Figure 14.

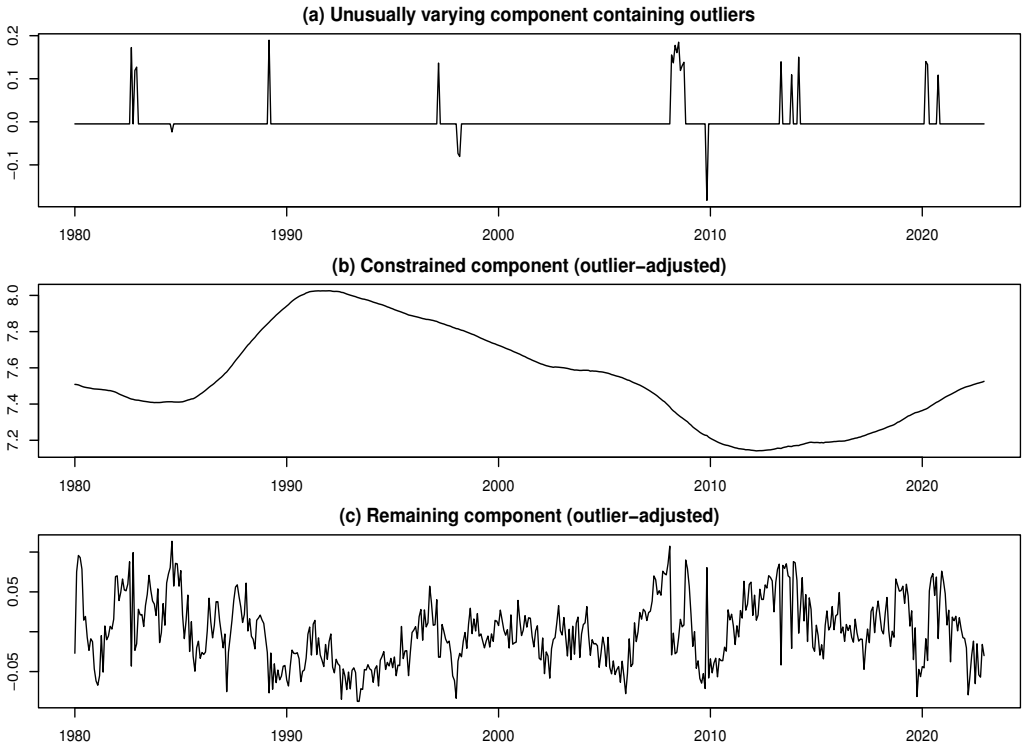

Figure 14. Decomposed results for log-transformed time series of W6.

Figure 14a shows a graph of the abnormal variation component, which contains outliers, of Building Materials (W6). As a result, a number of outliers were found. However, as noted above, most of them are of no particular significance. This suggests relative stability in the building materials type, with numerous outliers identified but no major economic upheavals.

In Figure 14b, the graph of the constrained component of Building Materials (W6) is depicted. It represents the long-term variation (i.e., the trend) of W6. Examining the period from the late 1980s to the early 1990s, we observe that active construction investment played a significant role in shaping trends in the Japanese economy, serving as a driving force behind the economic boom. This boom was largely influenced by easing monetary policies and comprehensive economic stimulus measures. Additionally, Japan's growing population at the time contributed to the upward trend during this period. Ref. [25] examined the macroeconomic effects of investment policies aimed at extending the life of expressways in Japan, using a stochastic Ramsey model. Their numerical analysis results suggest that implementing life-extension investment policies for expressways offers advantages in terms of reducing economic fluctuations. Furthermore, the gradual decline in levels from early 2009 and the abrupt increase during the early 2020s are significant. These fluctuations may signify underlying factors influencing economic trends. The downward trend in early 2009 suggests an economic recession due to the global financial crisis aggravated by the failure of Lehman Brothers in September 2008, while the upward trend since early 2020 may reflect, for example, an increase in demand for construction materials for coronavirus vaccination sites.

In Figure 14c, a graph of the remaining component of Building Materials (W6) is shown. This graph provides information on short-term variations (i.e., cyclical fluctuations)

of W6. A closer look at the behavior of the graph in Figure 14c reveals that the amplitude of the remaining component is smaller during the bubble economy period from the late 1980s to the early 1990s than during other periods. This can be interpreted as evidence that the cyclical fluctuation of W6 during the bubble period was relatively stable. Furthermore, the amplitude of the remaining component is not so large for the period from the mid-1990s to the mid-2000s from the overall perspective of the period under analysis. However, from the end of the 2000s onward, the amplitude of the remaining component changed sharply and significantly. This observation suggests that the global financial crisis triggered structural changes in the building materials sector.

4.8. Analyzing Time-Series Data for Chemicals (W7)

Here, we present the analysis results for the time-series data of log-WS for Chemicals (W7). The estimated parameters are as follows: $\widehat{k}_1 = 17$, $\widehat{k}_2 = 72$, $\widehat{k}_3 = 76$, and the estimated number of outliers is $\widehat{m} = 1$. The identified outlier corresponds to time point 483, which aligns with March 2020, during the period of the COVID-19 outbreak.

Figure 15 indicates graphs of seasonal component and seasonally adjusted data for the log-transformed time series of Chemicals (W7).

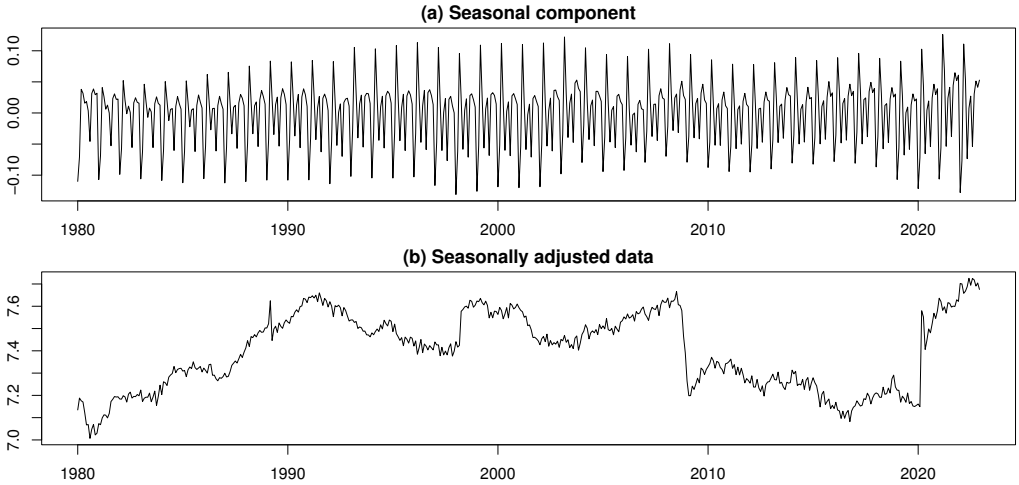

Figure 15. Seasonally adjusted results for log-transformed time series of W7.

By jointly observing the graphs in Figures 15a,b, we can confirm the following characteristics regarding the behavior of W7. First, focusing on Japan's bubble economy period, the graph of seasonally adjusted data in Figure 15b shows that W7 peaked in the early 1990s and began to decline. The graph of seasonal components in Figure 15a also shows a clear difference in seasonal variation between the periods before and after the early 1990s. In addition, the seasonally adjusted data graph in Figure 15b shows a sharp decline in W7 during the global financial crisis in the late 2000s, and the graph in Figure 15a also shows a change in the behavior of the seasonal variation during this period. Furthermore, turning to the period of the COVID-19 pandemic in the early 2020s, the seasonally adjusted data graph in Figure 15b shows a sharp rise in W7, and the graph in Figure 15a also clearly shows a change in the pattern of seasonal component variation during that period. Thus, we find evidence of the fact that the structure of the W7 sector has changed through time, i.e., there is evidence of the existence of structural change. In particular, the sharp increase in the wholesale sales of chemicals (W7) during the COVID-19 pandemic in the early 2020s can be regarded as an inevitable result of the social situation at that time.

Figure 16 depicts graphs of the unusually varying component, which contains outliers, the constrained component, and the remaining component for the log-transformed time series of Chemicals (W7), respectively.

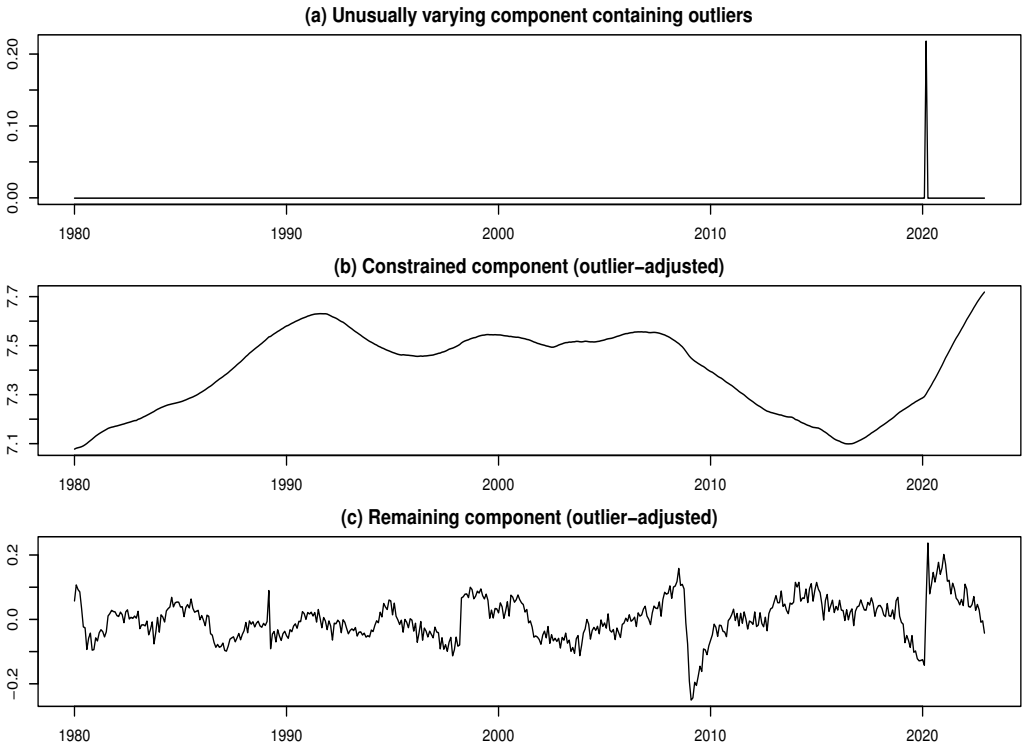

Figure 16. Decomposed results for log-transformed time series of W7.

Figure 16a depicts a graph of the unusually varying component. As a result, the only outlier is identified in early 2021. Needless to say, this period corresponds to the COVID-19 pandemic. Because of the extremely large shock of the COVID-19 pandemic around 2020, relatively minor levels of shocks may not have been detected as outliers. Moreover, Figure 16b depicts a graph of the constrained components for W7, from which we can see the trend in wholesale sales for W7. The main features of trend changes in this graph overlap with the discussion of the graph in Figure 15b above. To add a supplementary explanation, one reason for the significant increase in wholesale sales of chemicals in Japan in the early 2020s may be a reflection of the growing demand for quick-drying alcohol hand sanitizers in response to the COVID-19 pandemic. Furthermore, Figure 16c shows the graph of the remaining component. In terms of the behavior of the graph in Figure 16c, the short-term cyclical fluctuations for Chemicals (W7) are generally stable for the entire period under analysis. However, the period of the global financial crisis in the late 2000s and the COVID-19 pandemic in the early 2020s are characterized by exceptionally large amplitudes. This indicates that the impact of both shocks was extremely large.

4.9. Analyzing Time-Series Data for Minerals and Metals (W8)

In this section, we analyze the time-series data of log-WS for Minerals and Metals (W8). The parameter estimation results are as follows: $\widehat{k}_1 = 34$, $\widehat{k}_2 = 120$, $\widehat{k}_3 = 53$, and the estimated number of outliers is $\widehat{m} = 30$. The first 10 identified outlier locations correspond to time points 352, 353, 351, 343, 510, 350, 509, 354, 342, and 73.

Figure 17 shows graphs of seasonal component and seasonally adjusted data for the log-transformed time series of Minerals and Metals (W8).

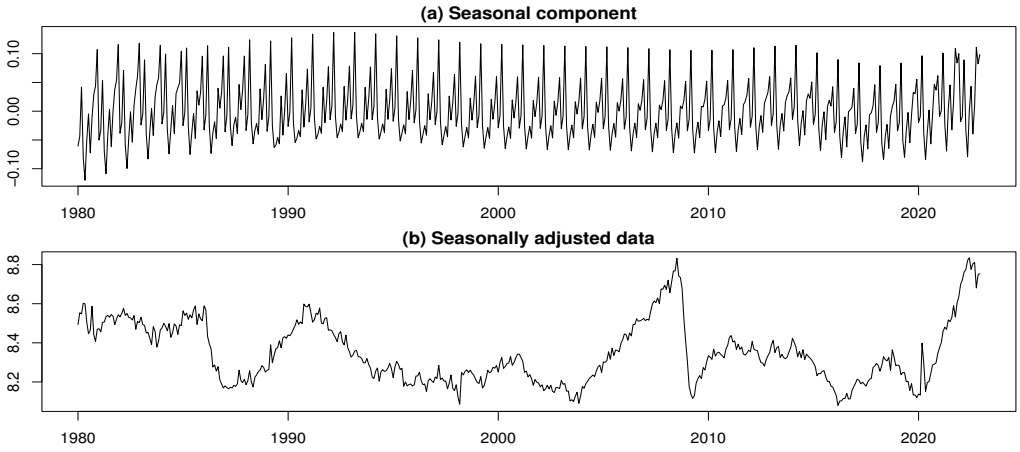

Figure 17. Seasonally adjusted results for log-transformed time series of W8.

We notice that the shapes of the graphs in Figure 17a and Figure 17b have many similarities with the cases in Figure 15a and Figure 15b, respectively. This suggests that the wholesale sales sectors of Chemicals (W7) and Minerals and Metals (W8) have similar structural characteristics. Observing the graph of seasonally adjusted data in Figure 17b, we can see that clear structural changes have occurred during the early 1990s, late 2000s, and early 2020s.

Figure 18 indicates graphs of the unusually varying component, which contains outliers, the constrained component, and the remaining component for the log-transformed time series of Minerals and Metals (W8), respectively.

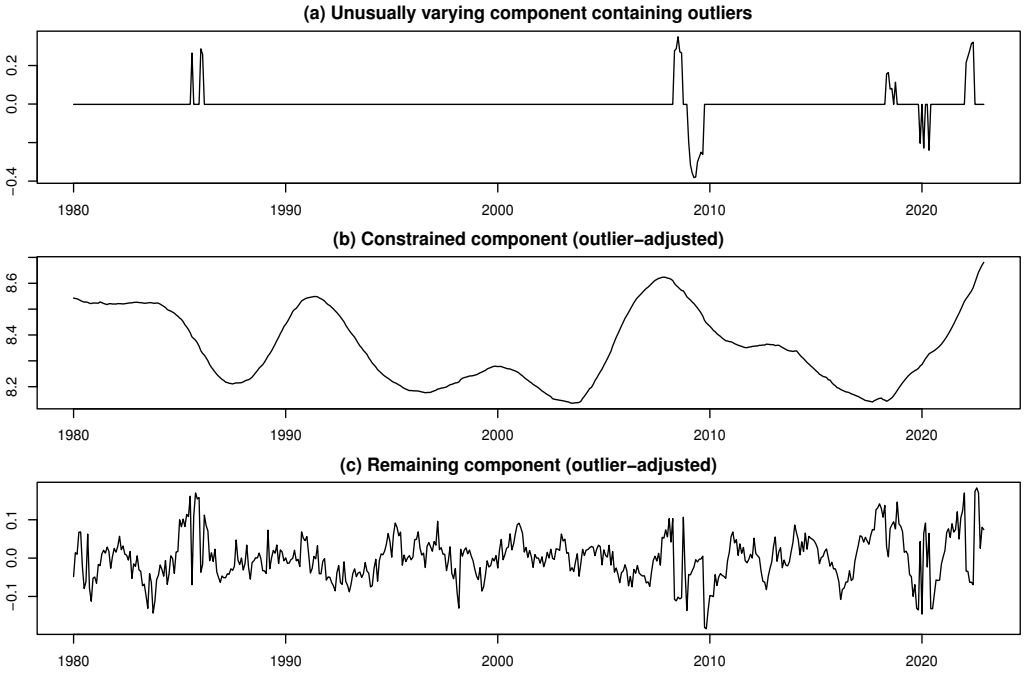

Figure 18. Decomposed results for log-transformed time series of W8.

From Figure 18a, we can see several outliers, but the decline in the late 2000s is particularly conspicuous. As has been mentioned many times in the previous discussions, this period corresponds to the global financial crisis. Figure 18b illustrates the trend in wholesale sales of W8 over the analysis period. The series shows pronounced peaks in the early 1990s and the late 2000s, as well as troughs in the late 1980s, the late 1990s, the early 2000s, and the late 2010s. Following the trough in the late 2010s, a sustained upward movement is observed, which may reflect a rapid increase in wholesale sales of

minerals and metals during the COVID-19 pandemic. These fluctuations suggest that the sector is strongly influenced by global commodity cycles, with periods of growth likely driven by rising international demand and price surges, and downturns corresponding to economic slowdowns and reduced industrial activity. The graph in Figure 18c shows the characteristics of short-term variation in W8. Some of the most striking features are the very large amplitudes of cyclical fluctuations in the mid-1980s, late 2000s, and early 2020s. It is clear that the amplitude increases in the late 2000s and early 2020s reflect the global financial crisis and the COVID-19 pandemic, respectively. According to the results reported in ([22], Ch. 4), both the stock price index (Nikkei 225) and the land price index for commercial land in Japan's six largest cities—Tokyo, Yokohama, Nagoya, Kyoto, Osaka, and Kobe—have increased sharply since 1985.

4.10. Analyzing Time-Series Data for Machinery and Equipment (W9)

In this subsection, we examine the time-series data of log-WS for Machinery and Equipment (W9). The parameter estimation results are as follows: $\widehat{k}_1 = 17$, $\widehat{k}_2 = 72$, $\widehat{k}_3 = 63$, and the estimated number of outliers is $\widehat{m} = 26$. The first 10 identified outlier locations correspond to time points 483, 351, 493, 494, 492, 495, 490, 353, 342, and 496.

Figure 19 depicts graphs of seasonal component and seasonally adjusted data for the log-transformed time series of Machinery and Equipment (W9).

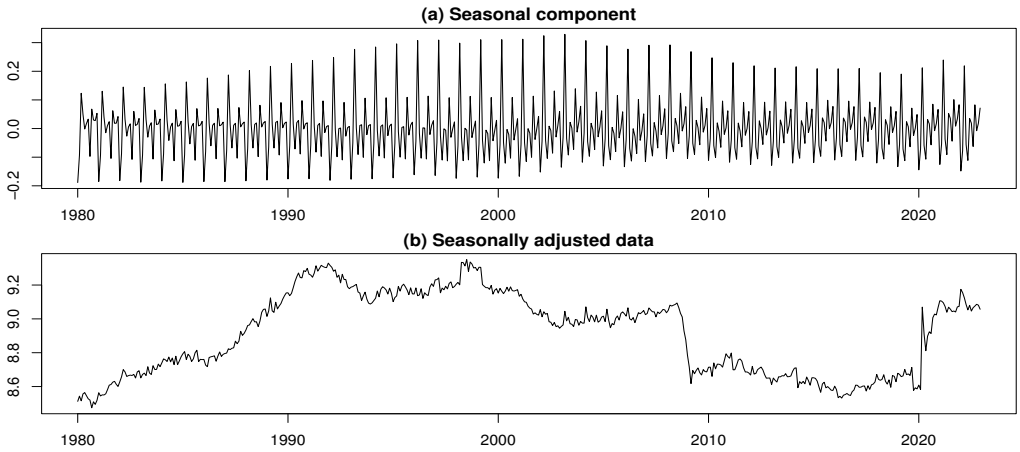

Figure 19. Seasonally adjusted results for log-transformed time series of W9.

For the graph of seasonally adjusted W9 data in Figure 19b, we notice a sharp drop in the late 2000s and a sharp rise in the early 2020s. Thus, wholesale sales of machinery and equipment plummeted in the late 2000s, which were affected by the global financial crisis. Conversely, in the early 2020s, the COVID-19 pandemic led to a sharp increase in wholesale sales of machinery and equipment. However, during most of the lost two decades of the Japanese economy from the early 1990s to the early 2010s, wholesale sales of machinery and equipment have been little affected by business fluctuations (with the exception of the global financial crisis in the late 2000s). The reason for this may be that the nature of machinery and equipment requires investment in maintenance and renewal at regular intervals.

Figure 20 displays graphs of the unusually varying component, which contains outliers, the constrained component, and the remaining component for the log-transformed time series of Machinery and Equipment (W9), respectively.

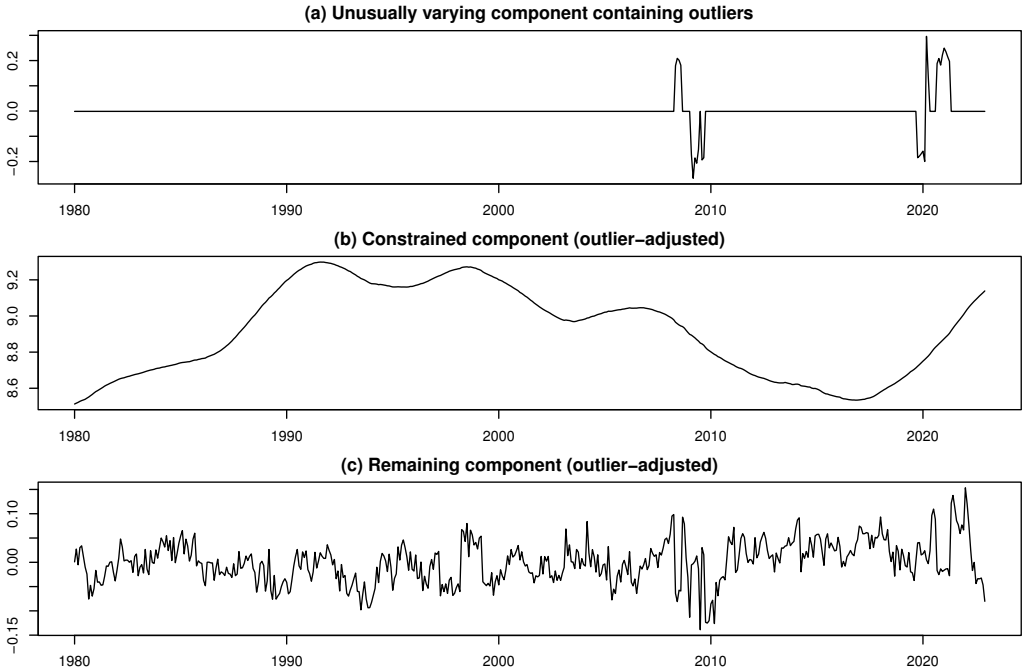

Figure 20. Decomposed results for log-transformed time series of W9.

Figure 20a depicts a graph of the unusually varying component of Machinery and Equipment (W9). As a result, two outliers were identified for the period of the late 2000s and early 2020s, respectively. These periods correspond to the global financial crisis and the COVID-19 pandemic, respectively. Since these events were extremely large shocks, it is possible that shocks of relatively minor levels were not detected as outliers. The graph of the constrained component of W9 in Figure 20b reveals a change over time in the trend of wholesale sales in W9. In particular, it is clear that the declining trend in the late 2000s and the rising trend in the early 2020s reflect the global financial crisis and the COVID-19 pandemic, respectively. The behavior of the residual component of W9 in Figure 20c shows that the amplitude of the cyclical variation of W9 is relatively large during the global financial crisis in the late 2000s and the COVID-19 pandemic in the early 2020s.

4.11. Analyzing Time-Series Data for Furniture and House Furnishings (W10)

In this section, we analyze the time-series data of log-WS for Furniture and House Furnishings (W10). The parameter estimation results are as follows: $\widehat{k}_1 = 16$, $\widehat{k}_2 = 36$, $\widehat{k}_3 = 38$, and the estimated number of outliers is $\widehat{m} = 26$. The first 10 identified outlier locations correspond to time points 483, 484, 490, 492, 486, 487, 493, 494, 491, and 488.

Figure 21 shows graphs of seasonal component and seasonally adjusted data for the log-transformed time series of Furniture and House Furnishings (W10).

Observing the graphs shown in panels (a) and (b) of Figure 21 for Furniture and House Furnishings (W10), we find that they are similar to the graphs in panels (a) and (b) of Figure 9 for Livestock and Qquatic Products (W4), respectively. This suggests the existence of a structural relationship between the W4 and W10 sectors.

The graph of the seasonally adjusted data in Figure 21b confirms the following characteristics. First, the seasonally adjusted value of W10 has been decreasing with small fluctuations since the turning point in the early 1990s, when the bubble burst in the Japanese economy. In addition, the seasonally adjusted value of W10 shows a sharp increase in the early 2020s. As is well known, during the COVID-19 pandemic, many Japanese firms, as in many other countries, changed their work patterns to include remote work from home,

and workers' telecommuting hours increased. This background may have contributed to the rapid increase in wholesale sales of furniture and home furnishings in the early 2020s.

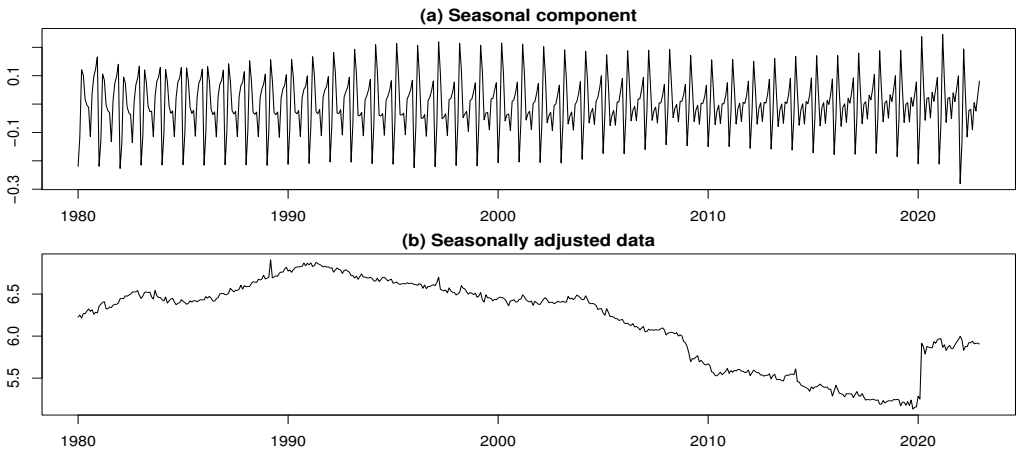

Figure 21. Seasonally adjusted results for log-transformed time series of W10.

Figure 22 depicts graphs of the unusually varying component, which contains outliers, the constrained component, and the remaining component for the log-transformed time series of Furniture and House Furnishings (W10), respectively.

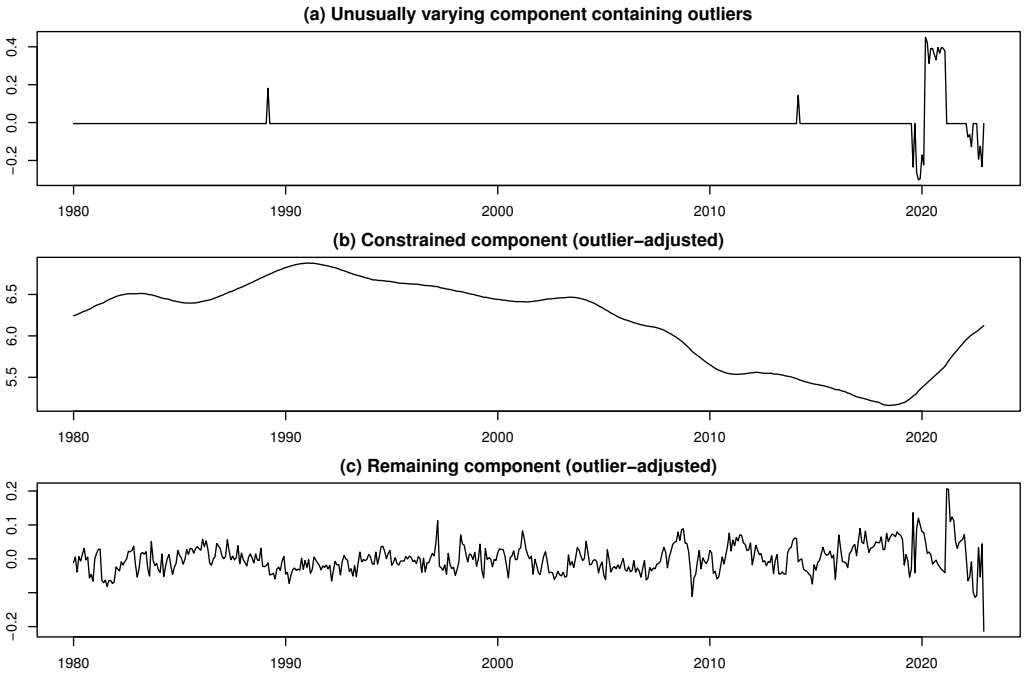

Figure 22. Decomposed results for log-transformed time series of W10.

The graph of unusually varying component in Figure 22a confirms the outlier that was prominent during the COVID-19 pandemic in the early 2020s. Moreover, Figure 22b shows that from the early 1990s to the end of the 2010s, the constrained component of W4 had a decreasing trend. However, from the early 2020s, the trend had turned sharply upward. This change in trend can be attributed to the increase in telecommuting hours of workers following the COVID-19 pandemic, as mentioned above. Furthermore, observing the behavior of the remaining component in Figure 22c, the cyclical pattern of variation appears to be relatively stable from the perspective of the entire period under analysis. However, as an exception, a large amplitude exists in the early 2020s. Clearly, this large amplitude reflects the impact of the COVID-19 pandemic.

4.12. Analysis of Time-Series Data for Medicines and Toiletries (W11)

This section is dedicated to analyzing the time-series data of log-WS for Medicines and Toiletries (W11). The estimated parameters are as follows: $\widehat{k}_1 = 23$, $\widehat{k}_2 = 108$, $\widehat{k}_3 = 46$, and the estimated number of outliers is $\widehat{m} = 1$. In other words, only one minor outlier was identified at time point 50.

Figure 23 depicts graphs of seasonal component and seasonally adjusted data for the log-transformed time series of Medicines and Toiletries (W11).

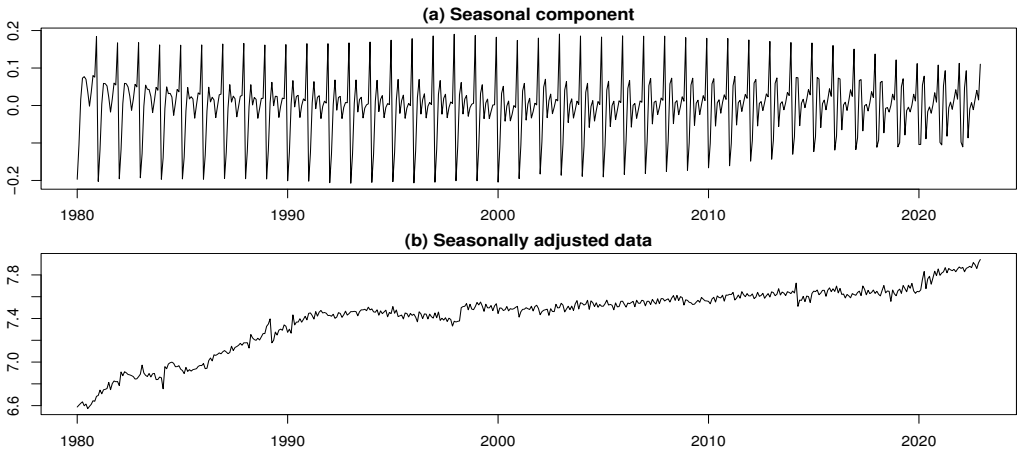

Figure 23. Seasonally adjusted results for log-transformed time series of W11.

Figure 24 indicates graphs of the unusually varying component, which contains outliers, the constrained component, and the remaining component for the log-transformed time series of Medicines and Toiletries (W11), respectively.

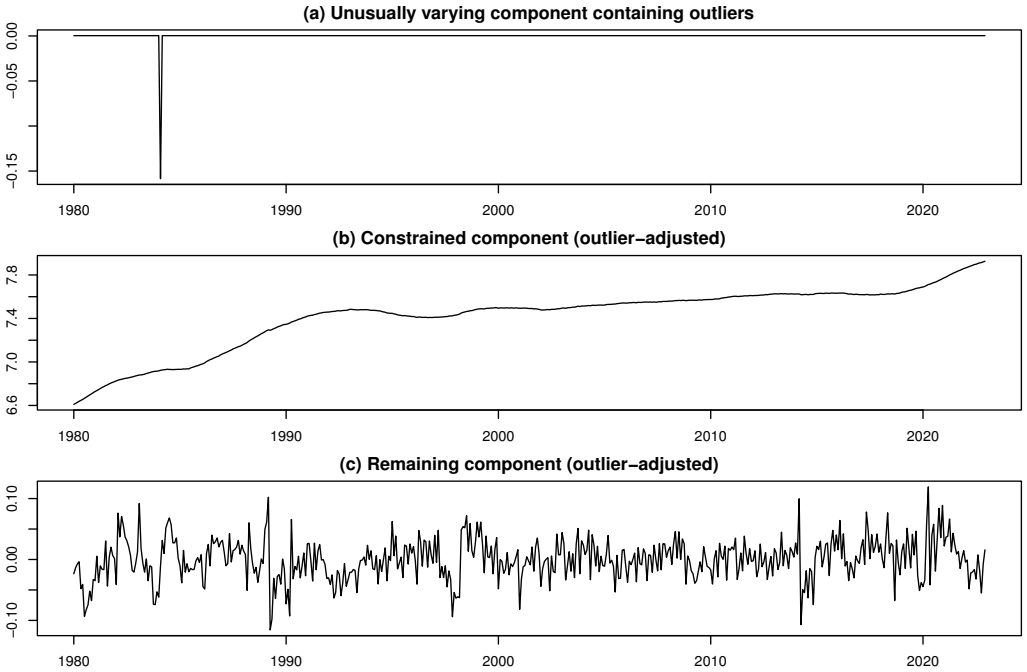

Figure 24. Decomposed results for log-transformed time series of W11.

From the graph of the unusually varying component of Figure 24a, the only outlier was identified in the period of the early 1980s. Figure 24b shows that the constrained component of Medicines and Toiletries (W11) increased almost consistently from the early 1980s to the early 2020s. Examining the behavior of the graph of the remaining component in Figure 24c, a relatively stable pattern of variation is observed for the cyclical fluctuations of wholesale

sales in W11. This result may be attributed to the fact that, as in the case of Food and Beverages (W5), Medicines and Toiletries (W11) are similar in nature to daily necessities.

4.13. Analysis of Time-Series Data for Others (W12)

In this section, we analyze the time-series of log-WS for the Others (W12) category. The parameter estimation results are as follows: $\widehat{k}_1 = 12$, $\widehat{k}_2 = 48$, $\widehat{k}_3 = 38$, and the estimated number of outliers is $\widehat{m} = 28$. The first 10 identified outlier locations correspond to time points 341, 479, 343, 380, 459, 461, 458, 219, 457, and 464; however, there are no distinctive or noticeable outliers.

Figure 25 depicts graphs of seasonal component and seasonally adjusted data for the log-transformed time series of Others (W12).

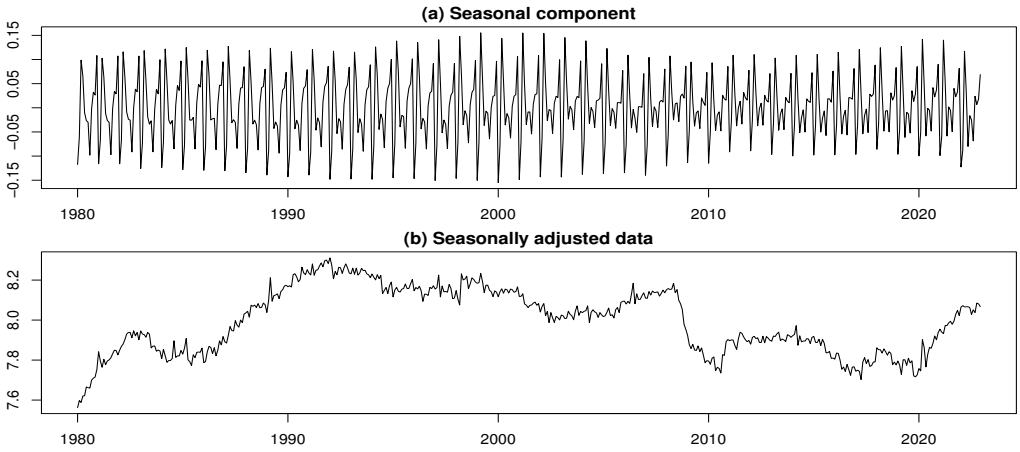

Figure 25. Seasonally adjusted results for log-transformed time series of W12.

The graph in panel (b) of Figure 25 shows differences in the behavior of seasonally adjusted data for the periods from the early 1980s to the late 1990s, from the early 1990s to the late 2000s, from the early 2010s to the late 2010s, and from the 2020s onward. In other words, the characteristics described above indicate structural changes in the wholesale sales of W12.

Figure 26a shows a graph of the unusually varying component, which contains outliers, of W12. As a result, a number of outliers were found. However, most of them can be interpreted to be of no particular significance. In Figure 26b, the graph of the constrained component of W12 is depicted. Looking at the period from the late 1980s to the early 1990s in Figure 26b, we find that W12 played an important role in shaping trends in the Japanese economy, serving as a driving force behind the boom. Moreover, we notice the gradual decline in levels from late 2000s and the abrupt increase during the early 2020s. Specifically, the downward trend in late 2000s implies a recession due to the global financial crisis, while the upward trend since early 2020 may reflect the COVID-19 pandemic. The graph of the remaining component of W12 in Figure 26c shows the short-term variations (i.e., cyclical fluctuations) of W12. A closer look at the behavior of the graph in Figure 20c reveals that the amplitude of the remaining component was smaller during the bubble economy period from the late 1980s to the early 1990s. This is evidence of the relatively stability of the cyclical fluctuations in W12 during the period of the bubble economy. Moreover, the amplitude of the remaining component is not so large for the period from the mid-1990s to the mid-2000s. Furthermore, since the end of the 2000s, the amplitude of the remaining component changed sharply and significantly. This suggests that the global financial crisis triggered structural changes in sector of W12.

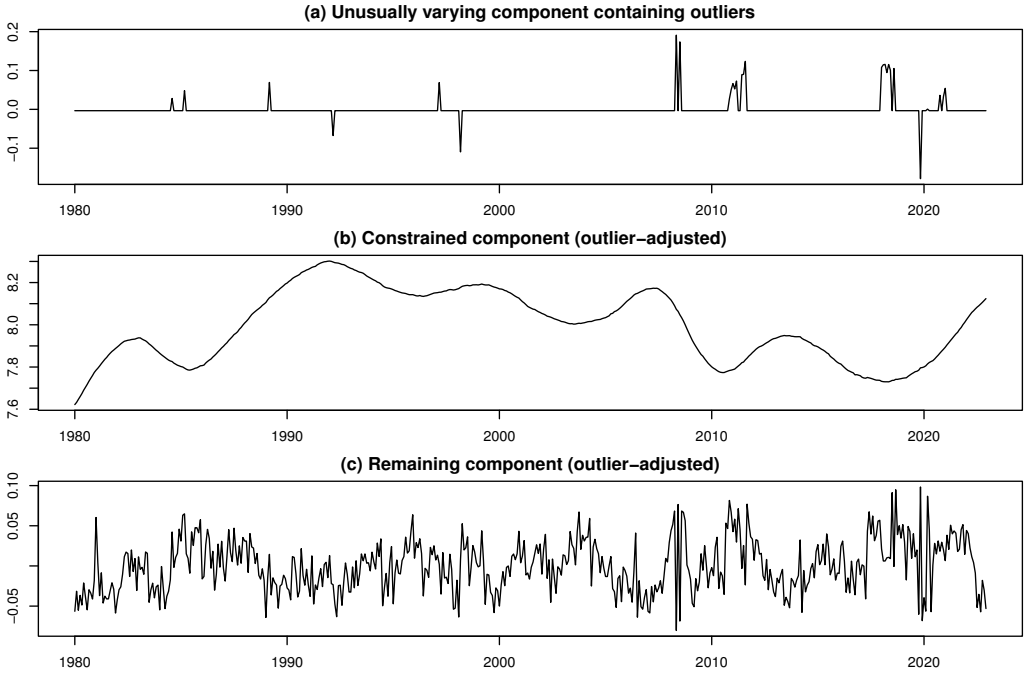

Figure 26. Decomposed results for log-transformed time series of W12.

5. Analysis of Dynamics of Impact from Business Cycles

In Section 4, we conducted component decomposition and analyzed the fluctuation characteristics of each type of wholesale sales in Japan from an economic perspective. However, due to the complexity of the variations in the remaining component, which contains cyclical variation, a comprehensive analysis could not be performed. While it is conceivable that this component is closely related to business cycles, considering that this relationship also varies over time, a newly proposed modeling approach will be employed in this section to analyze the dynamics of the impact from business cycles on each type of wholesale sales.

5.1. Another Extension of the ML Model

Let w_t represent the time series of the remaining component for a type of wholesale sales and u_t denote the time series for the composite index (CI), indicating the business cycles in Japan. Utilizing the component decomposition algorithm, we can assume that the global means of w and u are both zero. In this context, we examine the dynamics in the relation between the time series w_t and u_t using a linear model with a time-varying coefficient as follows:

$$w_t = a_n u_t + r_t \quad (t = 1, 2, \ldots, N). \tag{18}$$

In Equation (18), N represents the sample size mentioned in the preceding sentence, a_n denotes the unknown time-varying coefficient, where n varies with the time t, and r_t stands for the residual. Adhering to a common assumption in linear models, we assume the time series of the residual r_t to be stationary with a zero mean and independent of the explanatory variable u_t. No specific probability distribution is imposed on the residual, allowing its distribution to remain unrestricted. The time series of the residual may follow a certain model, allowing, for instance, the presence of serial correlation.

Essentially, the model in Equation (18) possesses the following characteristics: a dynamic covariance between the explanatory variable u_t and dependent variable w_t can be described through the time-varying coefficient a_n. Furthermore, there are no stringent constraints on the distribution of the residual series r_t, and no specific assumptions are

made regarding its variation patterns, aside from the mild assumption of stationarity. Consequently, this model is termed a dynamic linear model with distribution-free residuals or simply as the distribution-free dynamic linear (DFDL) model.

The DFDL model holds significant potential for analyzing relationships among economic variables, thanks to the dynamic and intricate nature of these connections. Nonlinear models, although capable of precisely representing such relationships, often pose identification challenges due to their limitless formulation, demanding considerable efforts in parameter estimation. Linear models, on the other hand, often serve as effective approximations for relationships among economic variables, allowing for the portrayal of dynamics through time-varying parameters. This strategy facilitates the approximation of complex relationships using simpler models, making it particularly suitable for the era of big data.

Considering scenarios where the time-varying coefficient a_n exhibits smoothness over time, assuming that the residual r_t follows a normal distribution allows for constructing a Bayesian linear model using the smoothness priors method (see [9]; see also [26]). This approach facilitates the estimation of the time-varying coefficient using Bayesian linear modeling or state-space modeling methods. However, it is crucial to note that these methods are not applicable to the DFDL model.

In this context, the ML approach proposed by [13] is applied to estimate the time-varying coefficient. To achieve this, each term in Equation (18) is multiplied by u_t to rewrite the DFDL model as follows:

$$w_t u_t = a_n u_t^2 + r_t u_t \quad (t = 1, 2, \ldots, N). \tag{19}$$

Therefore, by setting $y_t = w_t u_t$ and treating $s_t = a_n u_t^2$ as the constrained component and $f_t = r_t u_t$ as the remaining component, the DFDL model can be considered as a special case of the ML model. It is important to note that mathematically, Equations (18) and (19) are equivalent, but they lead to different results in statistical modeling, particularly in the estimation of the time-varying coefficient a_n. In Equation (18), where the explanatory variable u_t has a global mean of zero and fluctuates widely within a range that includes zero, this may lead the estimated values of the time-varying coefficient a_n to be unstable. In contrast, in Equation (19), $u_t^2 > 0$ plays as the explanatory variable and falls within a positive range. So, it can lead to stable estimates for the time-varying coefficient a_n. However, when we consider the model in Equation (19) as a linear model for the time-varying coefficient a_n, the probability distribution of the residual $f_t = r_t u_t$ may become more complex compared to the residual r_t in Equation (18). Nevertheless, the assumption that r_t is independent of u_t allows us to assume that the global mean of $f_t = r_t u_t$ is zero, satisfying the properties of the remaining component in the ML model approach. Additionally, in the ML model approach, there is no need for further stringent assumptions regarding the remaining component, making it convenient for applying the ML model approach to the model in Equation (19).

In accordance with the aforementioned scenario, we introduce a model as follows:

$$s_t = a_n u_t^2, \quad (t = n, n+1, \ldots, n+k-1). \tag{20}$$

Here, Equation (20) implicitly represents the constrained component s_t as a linear model of u_t^2 for a fixed value of n, with k denoting the width of the time interval $[n, n+k-1]$. Note that the value of n can be shifted as $n = 1, 2, \ldots, N-k+1$ for estimating the time-varying coefficient a_n. Essentially, by setting $\alpha_n = 0$, $\beta_n = a_n$, and substituting t with u_t^2 in Equation (2), the configuration in Equation (20) aligns with the original ML model setup. Therefore, under this configuration, with minor adjustments, the concepts and algorithms utilized in the original ML model approach can be applied.

It is crucial to emphasize that, within the context of Equation (20), for a given n, a_n is influenced by k observed data points within the interval $[n, n+k-1]$. As a result, for sufficiently large values of k, the value of a_n remains stable despite shifts in n, ensuring the smoothness of a_n. Similar to the ML model, the smoothness of a_n becomes more evident as k increases. Therefore, by substituting $y_t = w_t u_t$, $z_t = u_t^2$, and $f_t = r_t u_t$, the model in Equation (19) is expressed as

$$y_t = a_n z_t + f_t, \quad (t = n, n+1, \ldots, n+k-1), \tag{21}$$

or in vector form as

$$\boldsymbol{y}(n) = a_n \boldsymbol{z}(n) + \boldsymbol{f}(n), \tag{22}$$

where

$$\boldsymbol{y}(n) = \begin{bmatrix} y_{n+k-1} \\ y_{n+k-2} \\ \vdots \\ y_n \end{bmatrix}, \ \boldsymbol{z}(n) = \begin{bmatrix} z_{n+k-1} \\ z_{n+k-2} \\ \vdots \\ z_n \end{bmatrix}, \ \boldsymbol{f}(n) = \begin{bmatrix} f_{n+k-1} \\ f_{n+k-2} \\ \vdots \\ f_n \end{bmatrix} = \begin{bmatrix} f_1^{(n)} \\ f_2^{(n)} \\ \vdots \\ f_k^{(n)} \end{bmatrix},$$

and $\mathbf{1}_k$ denotes a k-dimensional vector in which all elements are 1. Note that the value of n in Equations (21) and (22) can be taken in the range between 1 and $N-k+1$.

Furthermore, we set

$$\boldsymbol{f}(n-1) = (f_{n+k-2}, f_{n+k-3}, \ldots, f_{n-1})^{\mathtt{t}} = (f_1^{(n-1)}, f_2^{(n-1)}, \ldots, f_k^{(n-1)})^{\mathtt{t}}$$

denoting the vector associated with the remaining component for $\boldsymbol{y}(n-1)$ in the $(n-1)$-th time interval. It can be observed that $f_j^{(n)}$ and $f_{j-1}^{(n-1)}$ represent the same term, namely, f_{n+k-j}, of the remaining component for $j = 2, 3, \ldots, k$. However, they may undergo slight changes to accommodate for $\boldsymbol{y}(n-1)$ and $\boldsymbol{y}(n)$ in the $(n-1)$-th and n-th time intervals. Thus, for a given value of n, the following relationship holds:

$$f_j^{(n)} = f_{j-1}^{(n-1)} + e_{n+1-j} \quad (j = 2, 3, \ldots, k), \tag{23}$$

where e_{n+1-j} represents the variation between $f_j^{(n)}$ and $f_{j-1}^{(n-1)}$.

Based on the settings described above, the model introduced earlier can be expressed as another extension of the ML model. Therefore, by making some adjustments, the ML model approach proposed by [13] can be applied.

5.2. Estimating the Time-Varying Coefficient

In Equation (22), the quantities a_n and $\boldsymbol{f}(n)$ are regarded as the parameters. To ensure stable parameter estimates, we adopt a Bayesian approach similar to that employed in the ML model approach.

First, we assume that a_n exhibits smooth variations with respect to n as

$$a_n = a_{n-1} + \varepsilon_n \tag{24}$$

under diffuse priors for ε_n. That is, we assume that $\varepsilon_n \sim \mathcal{N}(0, \eta^2)$ in Equation (24), where the variance η^2 can be set to a sufficiently large value.

Furthermore, to obtain stable estimates of the remaining component, based on the assumption that the global mean of f_t is zero, we assume local sum stationarity for it over the interval $[n, n+k-1]$, i.e., we introduce the following equation:

$$\sum_{j=1}^{k} f_j^{(n)} \approx 0. \tag{25}$$

Applying Equation (23) to the relations in Equation (25), we set

$$f_1^{(n)} = -\sum_{j=1}^{k-1} f_j^{(n-1)} + e_{n+k-1}. \tag{26}$$

Here, Equation (26) represents the priors for $f_1^{(n)}$. Moreover, we set

$$f_j^{(n)} = f_{j-1}^{(n-1)} + e_{n+k-j} \quad (j = 2, 3, \ldots, k). \tag{27}$$

Thus, the priors for $f_j^{(n)}$ with $j = 2, 3, \ldots, k$ are established by Equation (27).

In the above equations, $e_n, e_{n-1}, \ldots, e_{n-k+1}$ represent a set of system noises. It is assumed that $e_n \sim \mathcal{N}(0, \sigma^2)$ and $e_m \sim \mathcal{N}(0, \sigma^2)$ are independent for $m \neq n$, where σ^2 is regarded as an unknown parameter.

Moreover, we have the settings

$$\boldsymbol{x}_n = \begin{bmatrix} a_n \\ f_1^{(n)} \\ f_2^{(n)} \\ \vdots \\ f_k^{(n)} \end{bmatrix}, \quad \boldsymbol{F} = \begin{bmatrix} 1 & 0 & 0 & \cdots & \cdots & 0 \\ 0 & -1 & -1 & \cdots & \cdots & -1 \\ 0 & 1 & 0 & \cdots & \cdots & 0 \\ \vdots & 0 & \ddots & \ddots & & \vdots \\ \vdots & \vdots & \ddots & \ddots & \ddots & \vdots \\ 0 & 0 & \cdots & 0 & 1 & 0 \end{bmatrix}, \tag{28}$$

$$\boldsymbol{v}_n = \begin{bmatrix} \varepsilon_n \\ e_{n+k-1} \\ e_{n+k-2} \\ \vdots \\ e_n \end{bmatrix}, \quad \boldsymbol{G} = \boldsymbol{I}_{k+1}, \quad \boldsymbol{H}_n = \begin{bmatrix} \boldsymbol{z}(n) & \boldsymbol{I}_k \end{bmatrix}, \tag{29}$$

with $\boldsymbol{I}_k$ representing a k-dimensional unit matrix. Utilizing the settings described in Equations (28) and (29) along with $\boldsymbol{H} = \boldsymbol{H}_n$, a Bayesian form of the DFDL model can be expressed in a state-space form as Equations (13) and (14), where $\boldsymbol{v}_n \sim \mathrm{N}(\boldsymbol{0}, \boldsymbol{Q})$ with $\boldsymbol{Q} = \mathrm{diag}(\eta^2, \sigma^2, \ldots, \sigma^2)$.

Importantly, a key feature of the DFDL model in Equation (18) is that no specific probability distribution is imposed on the original residuals r_t; these residuals are incorporated into the remaining component f_t. In this framework, the temporal evolution of the remaining component is represented by stochastic difference equations, with the errors in these equations treated as system noise in a state-space formulation. However, these stochastic fluctuations of the errors do not reflect inherent temporal randomness but rather arise from shifts in the data window used for estimation (see [13]). For practical estimation and uncertainty quantification, we adopt a Gaussian state-space approximation and apply the Kalman filter; that is, we model the system noise as normally distributed in order to implement the filter and to construct confidence intervals for the estimated coefficients. This Gaussian assumption is therefore a pragmatic computational device and does not imply that the underlying DFDL model imposes any distributional restriction on the original residuals r_t. In other words, the model remains distribution-free with respect to r_t, while the Gaussian state-space approximation provides a convenient means of obtaining point estimates together with approximate measures of uncertainty.

Thus, the Kalman filter and fixed interval smoothing algorithms can be employed to estimate the time-varying coefficient a_n associated with the state vector $\boldsymbol{x}_n$. Consequently, the estimate $\widetilde{a}_n$ for a_n is derived as the first element in the vector $\boldsymbol{x}_{n|N}$ for $n = 1, 2, \ldots, N - k + 1$.

However, it is essential to align $\widetilde{a}_n; n = 1, 2, \ldots, N - k + 1$, the estimations derived from the Kalman filter, with $\widehat{a}_t; t = 1, 2, \ldots, N$, representing the final estimates for the time-varying coefficient. Initially, for $n = 1, 2, \ldots, N - k + 1$, since $\widetilde{a}_n$ in the interval $[n, n + k - 1]$ corresponds to $\widehat{a}_t$ at the midpoint of that interval, which is $t = \frac{k-1}{2} + n$, this means that if k is odd,

$$\left\{\widehat{a}_t; t = \frac{k-1}{2} + 1, \frac{k-1}{2} + 2, \ldots, \frac{k-1}{2} + N - k + 1\right\}$$

is set to $\{\widetilde{a}_n; n = 1, 2, \ldots, N - k + 1\}$, $\{\widehat{a}_t; t < \frac{k-1}{2} + 1\}$ is set to $\widetilde{a}_1$; and $\{\widehat{a}_t; t > \frac{k-1}{2} + N - k + 1\}$ is set to $\widetilde{a}_{N-k+1}$. Conversely, if k is even, there is no corresponding value at the midpoint $n + \frac{k-1}{2}$ of the interval. Thus, $\{\widehat{a}_t; t = \frac{k}{2} + 1, \frac{k}{2} + 2, \ldots, N - \frac{k}{2}\}$ is set to $\{\frac{\widetilde{a}_n + \widetilde{a}_{n+1}}{2}; n = 1, 2, \ldots, N - k\}$, $\{\widehat{a}_t; t < \frac{k}{2} + 1\}$ is set to $\frac{\widetilde{a}_1 + \widetilde{a}_2}{2}$, and $\{\widehat{a}_t; t > N - \frac{k}{2}\}$ is set to $\frac{\widetilde{a}_{N-k} + \widetilde{a}_{N-k+1}}{2}$.

5.3. Method for Estimating the Parameters

In the DFDL model, the width of the time interval, denoted by k, and the variance of the system noises, represented by σ^2, are crucial parameters. To estimate these parameters, a likelihood function for the original ML model was defined in [13]. However, since the likelihood function for the DFDL model differs slightly from that of the original model, we provide the following outline of the estimation method for the associated parameters for users of the DFDL modeling approach.

Following [7], the density function for $\boldsymbol{y}(n)$ is a normal density given by

$$g(\boldsymbol{y}(n)|\sigma^2, k) = \frac{1}{\sqrt{(2\pi\sigma^2)^k |\boldsymbol{U}_{n|n-1}|}} \exp(-\frac{S^2(n)}{2\sigma^2})$$

based on the Kalman filter, where

$$S^2(n) = (\boldsymbol{y}(n) - \boldsymbol{y}_{n|n-1})^{\mathsf{t}} \boldsymbol{U}_{n|n-1}^{-1} (\boldsymbol{y}(n) - \boldsymbol{y}_{n|n-1})$$

with $\boldsymbol{y}_{n|n-1}$ and $\boldsymbol{U}_{n|n-1}$ being the mean and covariance of $\boldsymbol{y}(n)$, which are given by

$$\boldsymbol{y}_{n|n-1} = \boldsymbol{H}_n \boldsymbol{x}_{n|n-1}, \quad \boldsymbol{U}_{n|n-1} = \boldsymbol{H}_n \boldsymbol{V}_{n|n-1} \boldsymbol{H}_n^{\mathsf{t}},$$

where $\boldsymbol{x}_{n|n-1}$ and $\boldsymbol{V}_{n|n-1}$ are the mean and the covariance matrix for the state vector $\boldsymbol{x}_n$ in the prediction step of the Kalman filter. Moreover, we structure $\boldsymbol{y}(n)$, $\boldsymbol{y}_{n|n-1}$, $\boldsymbol{x}_{n|n-1}$, $\boldsymbol{V}_{n|n-1}$, and $\boldsymbol{H}_n$ as follows:

$$\boldsymbol{y}(n) = \begin{bmatrix} y_{n+k-1} \\ \boldsymbol{y}^{(1)}(n) \end{bmatrix}, \quad \boldsymbol{y}_{n|n-1} = \begin{bmatrix} \widehat{y}_{n+k-1} \\ \boldsymbol{y}^{(1)}_{n|n-1} \end{bmatrix}, \quad \boldsymbol{V}_{n|n-1} = \begin{bmatrix} a & \boldsymbol{b}^{\mathsf{t}} \\ \boldsymbol{b} & \boldsymbol{V}^{(1)}_{n|n-1} \end{bmatrix}, \quad \boldsymbol{H}_n = [\boldsymbol{h}_n | \boldsymbol{H}_n^*]$$

with a and $\boldsymbol{b}$ denoting an eligible quantity and an eligible vector, respectively. Then, the density function for $\boldsymbol{y}^{(1)}(n)$ is a normal density given by

$$g_1(\boldsymbol{y}^{(1)}(n)|\sigma^2, k) = \frac{1}{\sqrt{(2\pi\sigma^2)^{k-1} |\boldsymbol{U}^{(1)}_{n|n-1}|}} \exp(-\frac{S_1^2(n)}{2\sigma^2}).$$

where

$$S_1^2(n) = (\boldsymbol{y}^{(1)}(n) - \boldsymbol{y}_{n|n-1}^{(1)})^{\mathsf{t}}(\boldsymbol{U}_{n|n-1}^{(1)})^{-1}(\boldsymbol{y}^{(1)}(n) - \boldsymbol{y}_{n|n-1}^{(1)}), \quad \boldsymbol{U}_{n|n-1}^{(1)} = \boldsymbol{h}_n \boldsymbol{V}_{n|n-1}^{(1)} \boldsymbol{h}_n^{\mathsf{t}}.$$

Therefore, for $n = 1$, the joint density function of $Y_{1:k}$ is defined by $g(\boldsymbol{y}(1)|\sigma^2, k)$, and for $n = 2, 3, \ldots, N-k+1$, the density function for y_{n+k-1} conditionally on $\boldsymbol{y}^{(1)}(n)$ is given by

$$g_2(y_{n+k-1}|\boldsymbol{y}^{(1)}(n), \sigma^2, k) = \frac{g(\boldsymbol{y}(n)|\sigma^2, k)}{g_1(\boldsymbol{y}^{(1)}(n)|\sigma^2, k)} \quad (n = 2, 3, \ldots, N-k+1).$$

Thus, the joint density function for $Y_{1:N}$ can be given as follows:

$$L(\sigma^2, k|Y_{1:N}) = g(\boldsymbol{y}(1)|\sigma^2, k) \prod_{n=2}^{N-k+1} g_2(y_{n+k-1}|\boldsymbol{y}^{(1)}(n), \sigma^2, k). \tag{30}$$

When the observations for $Y_{1:N}$ is given, the function $L(\sigma^2, k|Y_{1:N})$ given in Equation (30) can be regarded as the likelihood for the parameters σ^2 and k; hence, the log-likelihood, $\mathrm{LL}(\sigma^2, k) = \log(L(\sigma^2, k|Y_{1:N}))$, is expressed as

$$\begin{aligned} \mathrm{LL}(\sigma^2, k) &= \log g(\boldsymbol{y}(1)|\sigma^2, k) + \sum_{n=2}^{N-k+1} \log g_2(y_{n+k-1}|\boldsymbol{y}^{(1)}(n), \sigma^2, k) \\ &= -\frac{N}{2}\log(2\pi\sigma^2) - \frac{1}{2}\{\log|\boldsymbol{U}_{1|0}| + \sum_{n=2}^{N-k+1}(\log|\boldsymbol{U}_{n|n-1}| - \log|\boldsymbol{U}_{n|n-1}^{(1)}|)\} \\ &\quad -\frac{1}{2\sigma^2}\{S^2(1) + \sum_{n=2}^{N-k+1}(S^2(n) - S_1^2(n))\} \end{aligned} \tag{31}$$

Therefore, for a given value of k, by maximizing the log-likelihood in Equation (31), the maximum likelihood estimator for σ^2 can be obtained analytically by

$$\widehat{\sigma}^2 = \frac{1}{N}\{S^2(1) + \sum_{n=2}^{N-k+1}(S^2(n) - S_1^2(n))\}.$$

Then, the conditional maximum log-likelihood is calculated by $\mathrm{LL}(\widehat{\sigma}^2, k)$, which depends only on the value of k. Thus, we can determine the value of k by maximizing the value of $\mathrm{LL}(\widehat{\sigma}^2, k)$.

6. Second Illustrative Example

In this example, to assess the impacts of business cycles on wholesale sales, we examine the dynamics of the relationship between the cyclical component, as derived in the initial illustrative example, for each type of wholesale sales, and the cyclical component of the coincident composite index (CI) in the Japanese economy.

6.1. Components Decomposition of CI

The dataset for Japan's coincident CI is available from the website of Economic and Social Research (https://www.esri.cao.go.jp/en/stat/di/di-e.html, accessed on 1 May 2023) within the Cabinet Office of the Japanese government. These data represent a monthly time series spanning from January 1985 to December 2022, covering a total of $N = 456$ months. Similar to the processing of the aforementioned wholesale sales data, we also applied a logarithmic transformation to the CI data. We refer to the logarithmic CI as log-CI. Figure 27 displays the time series plot for the log-CI.



Figure 27. log-CI time series in Japan (January 1985 to December 2022).

The use of the extended ML model approach for decomposing the time-series data for log-CI allows us to delineate the components comprising an unusually varying component containing outliers, a constrained component, and a remaining component. In this instance, the estimated width of the time interval is $\widehat{k} = 37$, and the estimated number of outliers is $m = 12$. Figure 28 presents the results of this decomposition for reference.

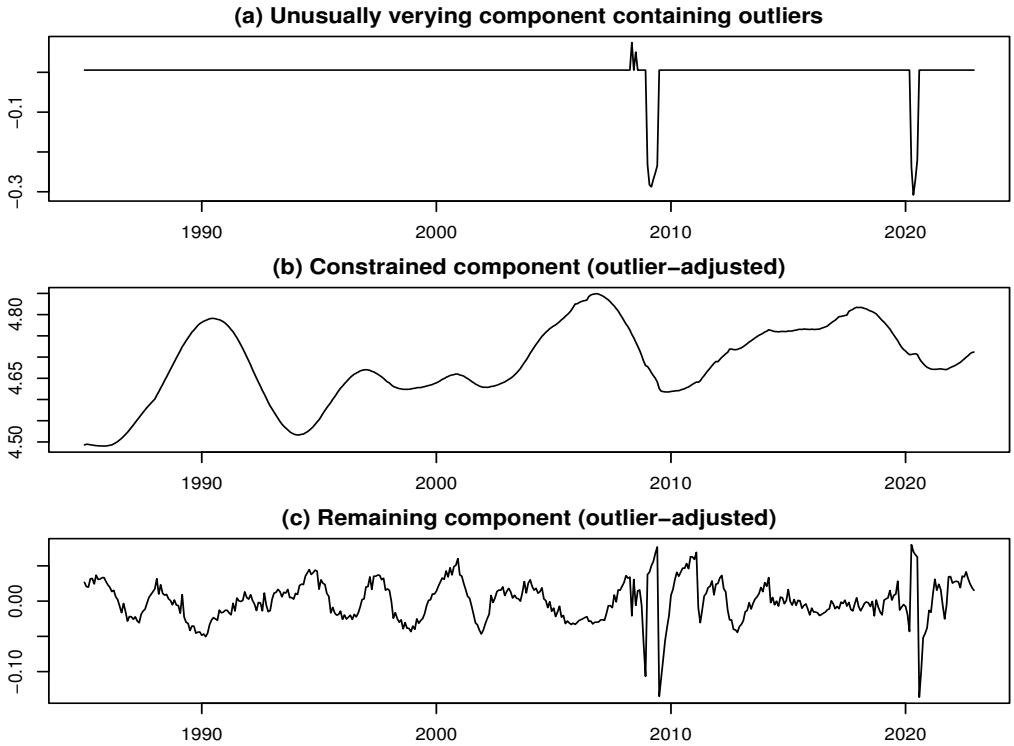

Figure 28. Decomposed results for the time series of log-CI.

The outliers evident in Figure 28a stand out prominently. Specifically, those occurring around 2009 are attributed to the aftermath of the global financial crisis, while those around 2021 are reflective of the impact of the COVID-19 pandemic. Figure 28b indicates the long-term fluctuations of the CI, representing the overall trend. It is important to emphasize that this graph captures the trend component of the CI. Conversely, Figure 28c portrays the short-term fluctuations, representing the remaining component after removing the trend. Essentially, this remaining component in Figure 28c signifies the cyclical variation in log-CI, where the trend has been extracted to highlight growth cycles (see, for details, [27]; see also [12]). Consequently, in this study, to analyze the impacts of business cycles on the remaining component in each type of wholesale sales, we utilized the remaining component in the log-CI as an explanatory variable.

6.2. Analyzing the Dynamics in the Relationship

In constructing individual DFDL models, we utilized the remaining component in each type of wholesale sales data as the dependent variable, denoted as w_t, and the remaining component in the log-CI data as the explanatory variable, denoted as u_t. It is essential to note that in each model, w_t and u_t were standardized to have a variance of 1, ensuring that the time-varying coefficients a_n approximately represent the correlation between w_t and u_t. Moreover, for parameter estimation, we leveraged monthly time-series data in the period from January 1985 to December 2022 for each variable, aligning with the sample period of the log-CI.

The estimated values of k for each type of model are 43, 40, 37, 35, 34, 36, 51, 34, 50, 34, 40, and 46, respectively.

The estimation of time-varying coefficients was carried out using the Kalman filter. Since these coefficients are random variables that evolve over time, it is important to assess the statistical significance of their fluctuations. Fortunately, the Kalman filter provides not only the estimated mean but also the variance of the time-varying coefficients. Therefore, in addition to the mean estimates, we computed the range of the mean plus or minus two standard deviations. At each point in time, the significance of a coefficient can be evaluated by examining the position of this range relative to the zero level. As illustrated in the figures below, the estimated time-varying coefficients are shown along with their mean ± 2 standard deviation bands, allowing for a straightforward assessment of both their significance and variability.

Figure 29 presents the estimated time-varying coefficients for each model (W1–W4). In each panel, the mean is depicted by a thick solid line, its ± 2 standard deviation band by thin solid lines, and the zero level by a dashed line.

Figure 29a shows a clear positive correlation between the wholesale sales of General Merchandise (W1) and the state of the economy. For the period from the mid-1980s to the early 1990s , a weak negative correlation between wholesale sales of general merchandise and the state of economy is observed. For periods other than the above, the correlation between the two appears to fluctuate in the neighborhood of zero.

For the wholesale sales value of Textiles (W2) in Figure 29b, a positive correlation with business conditions is noticeable in the period from the late 1980s to the early 1990s. However, there are weak negative correlations between wholesale sales value of textiles and the state of the economy the period from the early 1990s to the mid-1990s and the mid-1990s, respectively. For the other periods, there is almost no clear correlation between the two.

In Figure 29c, focusing on the wholesale sales value of Apparel and Sccessories (W3), there is a positive correlation with business conditions from the late 1980s to the early 1990s. Conversely, from the mid-1990s to the early 2000s, there was a negative correlation with the state of the economy. A positive correlation reemerges in the mid-2000s, with a subsequent period of little relationship between wholesale sales of apparel and accessories and business conditions from the late 2000s to the early 2010s. The relationship becomes complex from the mid-2010s to the late 2010s, and from the 2020s onwards, there is almost no correlation between both sides.

Examining Figure 29d, the relationship between the wholesale sales value of Livestock and Aquatic Products (W4) and business conditions appears complex. There is a weak positive correlation during the late 1980s to the early 1990s, followed by a period of little relationship during the mid-1990s, possibly reflecting the shock caused by the Great Hanshin-Awaji Earthquake in January 1995. Focusing on the latter half of the 1990s, a negative correlation emerges, followed by a return to a positive correlation for most of the 2000s. However, towards the end of the 2000s, there is little relationship between both

sides. A weak positive correlation reappears in the first half of the 2010s, followed by a strong negative correlation in the second half of the 2010s. In the 2020s, there is almost no correlation between both sides.

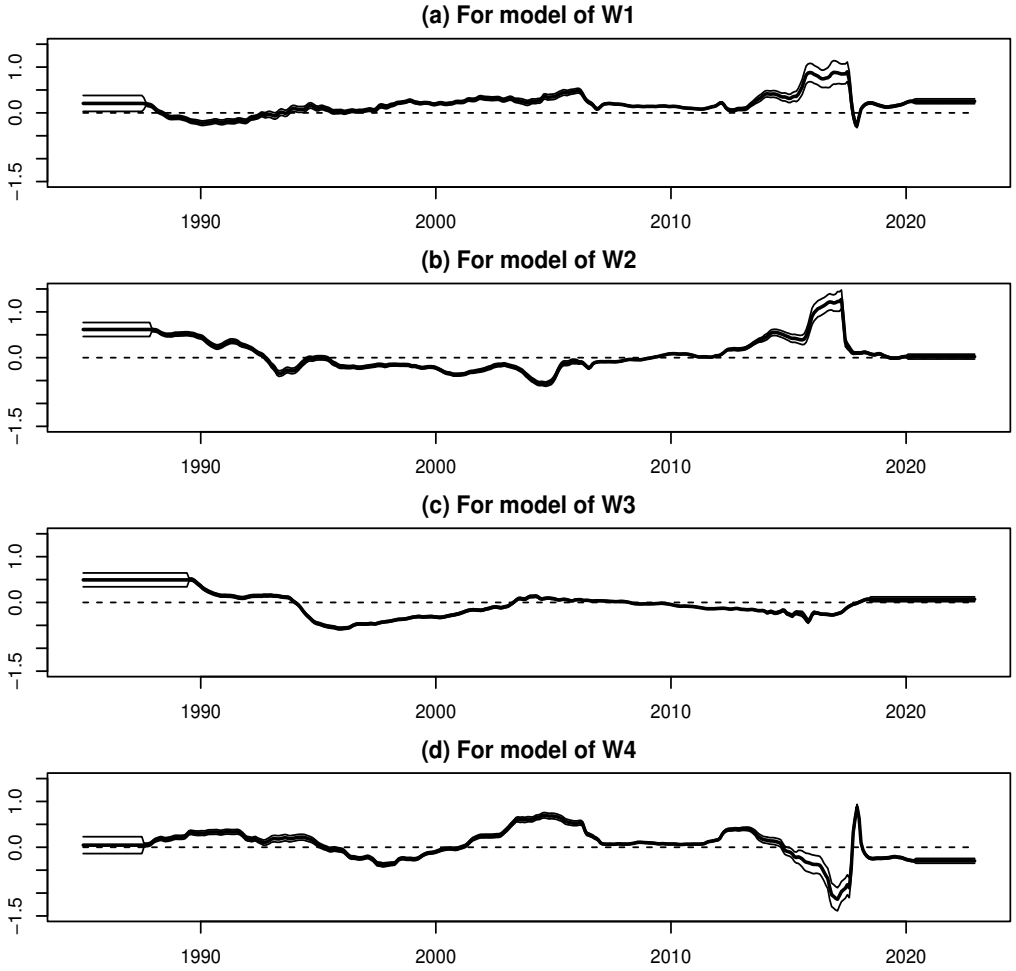

Figure 29. Estimation results for time-varying coefficients in the models for W1–W4.

Figure 30 depicts the graph of the estimated values of the time-varying coefficients in each model for W5–W8.

Regarding the wholesale sales value of Food and Beverages (W5), Figure 30a shows that there is a positive correlation with business conditions during the late 1980s and early 1990s. However, for the period from the mid-1990s to the late 1990s, there is a negative correlation, possibly influenced by the Great Hanshin-Awaji Earthquake. There is a positive correlation during the relatively short period of the mid-2000s. Since the late 2010s, there is almost no correlation between both sides.

As for the wholesale sales value of Building Materials (W6) in Figure 30b, there is a positive correlation from the late 1980s to the early 1990s, followed by a shift to a negative correlation during the period of the mid-1990s. Subsequently, a positive relationship exists during the relatively short period of the mid-2010s. However, a negative correlation reemerges in the period of the late 2010s. Since 2020, no clear relationship can be confirmed between both sides.

In Figure 30c, examining the wholesale sales value of Chemicals (W7) reveals a pattern similar to Building Materials (W7). There is a positive relationship from the mid-1980s to the early 1990s, followed by a negative correlation the during the period of late 1990s. For the period from the early 2000s to the mid-2010s, the correlation between the two appears to fluctuate in the neighborhood of zero. Subsequently, a negative correlation reemerges in

the relatively short period of the late 2010s. Since 2020, there is little relationship between both sides, resembling the case of W6.

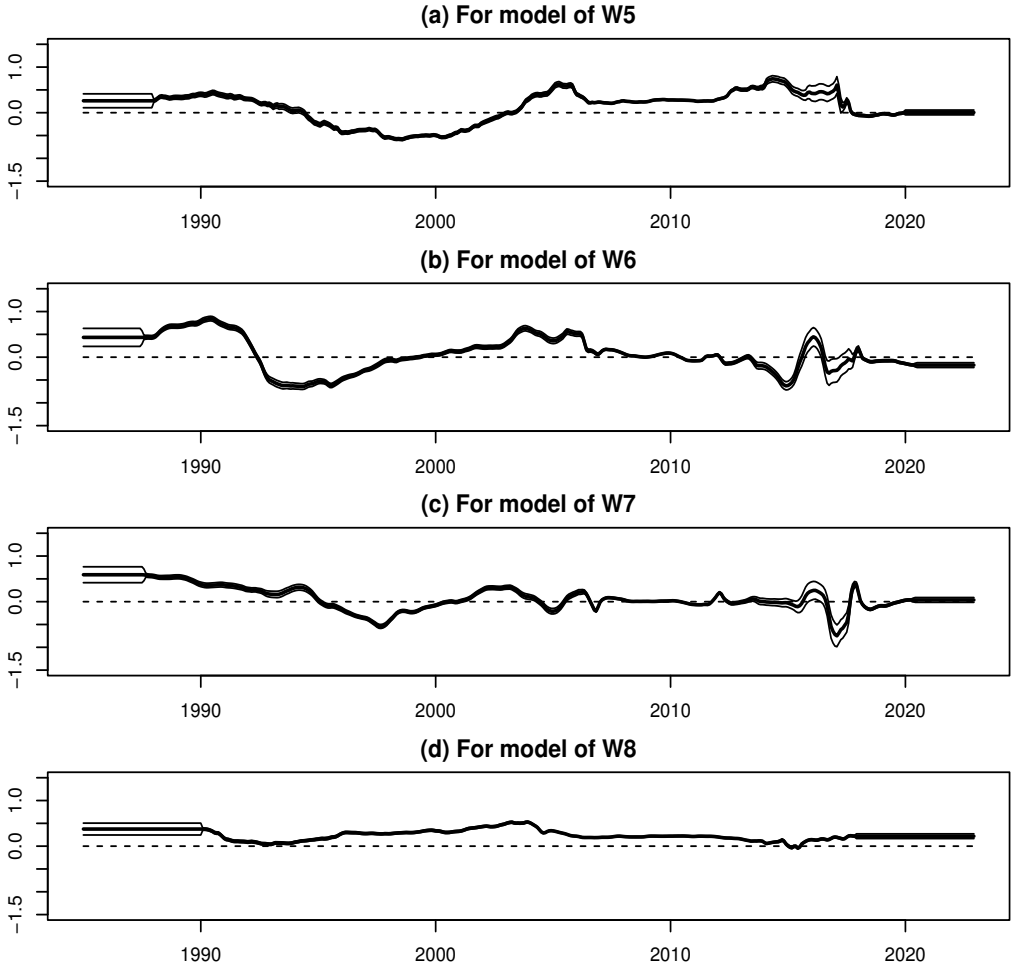

Figure 30. Estimation results for time-varying coefficients in the model for W5–W8.

Observing the relationship between the wholesale sales value of the minerals and metals (W8) and business conditions in Figure 30d, a clear positive correlation is evident in the late 1980s. However, the correlation between both sides remained almost zero during the period from the early 1990s to the mid-1990s. The correlation between both sides during the period from the late 1990s to the mid-2010s is complex, with repeated weak positive and negative correlations. There is a strong negative correlation in the period of the late 2010s. Since 2020, the relationship between both sides returned to almost zero correlation.

Figure 31 indicates the graph of estimated values of the time-varying coefficients in each model for W9–W12.

Examining Figure 31a, we find that there is a mild positive correlation between the wholesale sales value of Machinery and Equipment (W9) and business conditions in the period from the late 1980s to the early 1990s. However, for the period from the mid-1990s to the late 1990s, the relationship becomes weakly negative. For period from the early 2000s to mid-2010s, the correlation between both sides appears to fluctuate in the neighborhood of zero. For the period of the late 2010s, a relatively strong negative correlation between both sides can be confirmed. Since 2020s, there is almost no clear relationship between both sides.

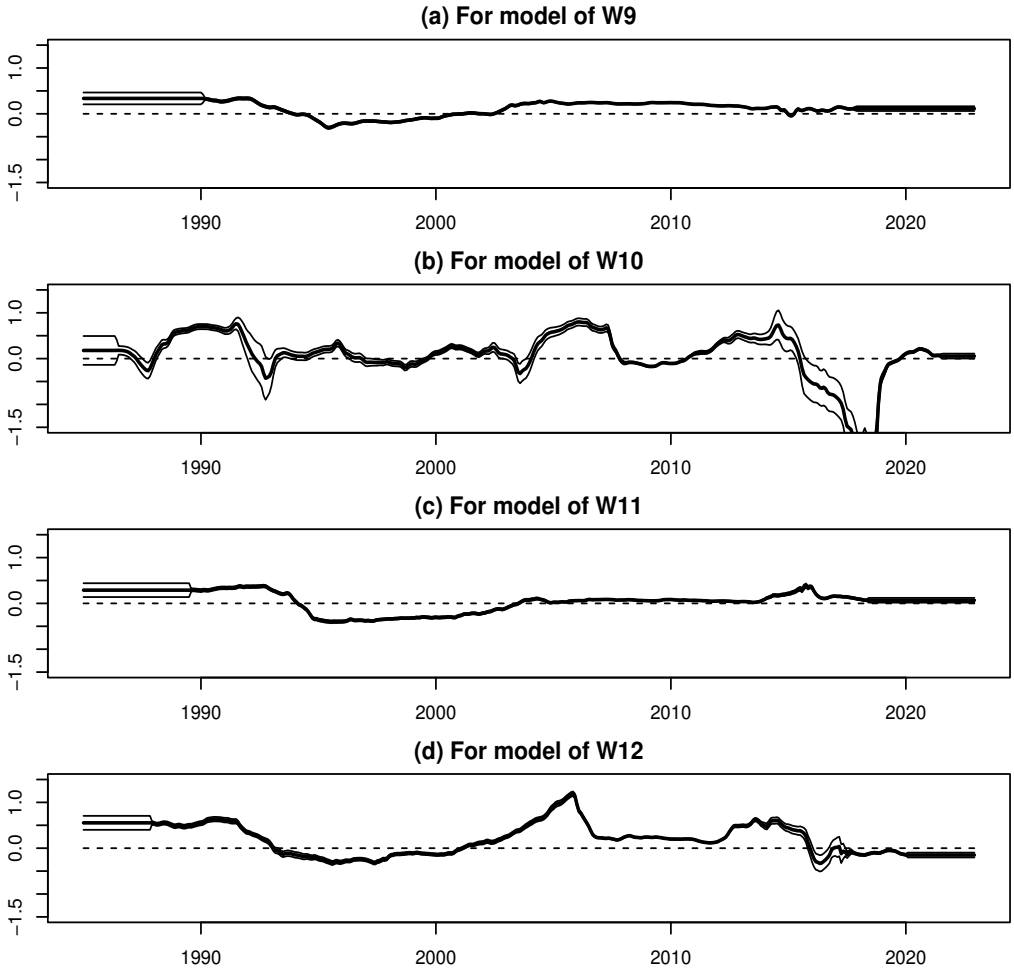

Figure 31. Estimation results for time-varying coefficients in the models for W9–W12.

Looking at the wholesale sales value of Furniture and House Furnishings (W10) in Figure 31b, there is a relatively strong positive correlation in the period from the late 1980s to the early 1990s. However, from the mid-1990s to the early 2000s, there is almost no relationship between both sides. A positive correlation reemerges in the mid-2000s. For the period from the early 2010s to the mid-2010s, we find that there is a mild positive correlation between the wholesale sales value of W10 and business conditions. A strong negative correlation between the two is observed from the mid-2010s to the late 2010s. In the 2020s, there is almost no correlation between both sides.

Observing the relationship between wholesale sales value of Medicines and Toiletries (W11) in Figure 31c, a weak negative correlation can be confirmed in the period of the late 1980s. A positive correlation is evident from the early 1990s, followed by a weakening of the relationship and a subsequent negative correlation until the early 2000s. In the mid-2000s, there is a mild positive correlation between both sides. For the period from the late 2000s to the early 2010s, the correlation between both sides appears to fluctuate in the neighborhood of zero. Thereafter, the correlation is negative in the mid-2010s period and turns positive in the late 2010s period. However, the correlation between the two has remained almost zero since the 2020s.

For the relationship between the wholesale sales value of Others (W12) and business conditions in Figure 31d, there is a positive correlation from the late 1980s to the early 1990s, followed by a weak negative correlation during the period of mid-1990s. From the late 1990s to the early 2010s, there is almost no relationship between both sides. A clear positive correlation is observed in the mid-2000s period. The correlation between the two is again

almost zero from the late 2000s to the early 2010s. Specifically, a positive correlation exists from the early 2010s to the mid-2010s, and a weak negative correlation is observed in the relatively short period during the late 2010s. After that, the correlation between the two is almost zero for the period from the 2020s onward.

To summarize, the strength and direction of the correlation between each type of wholesale sales value and the state of the economy vary over time. In other words, we presented evidence that the relationship between the wholesale sales for each business type and the state of the economy is not invariant. This relationship is influenced by macroeconomic conditions, government policies, and exogenous shocks. For instance, during major shocks like the global financial crisis or the COVID-19 pandemic, the correlation was shown to weaken significantly or become unclear. Despite this, the impact of certain events, like the Great East Japan Earthquake in March 2011, may not always be clearly reflected in these relationships, suggesting lessons learned from past experiences.

7. Summary and Discussion

This section provides a comprehensive overview and discussion of the main findings and implications presented in the preceding sections.

In Section 3, we conducted an extensive review of the ML model approach introduced by [13], along with its extended versions by [14,19]. These methodologies offer an extended ML model framework for decomposing monthly time-series data into constrained, remaining, seasonal, and outlier components. In Section 4, we applied the extended ML model approach discussed in Section 3 to decompose the time-series data of 12 types of wholesale sales in Japan. This decomposition enabled a detailed analysis of the structural dynamics within each type of wholesale sales, allowing for a nuanced examination of their behavior over time. Our analysis revealed the existence of structural changes in the majority of the wholesale sales sector, which were triggered by the collapse of the Japanese bubble economy in the early 1990s, the global financial crisis in the late 2000s, and the COVID-19 pandemic in the early 2000s. In Section 5, we constructed a DFDL model to investigate the dynamic effect of business cycles on each type of wholesale sales. To estimate the time-varying coefficients in the DFDL model, we proposed an additional extension of the ML model approach. Based on the estimated time-varying coefficients, we analyzed the socio-economic impacts on each type of wholesale sales across different periods. In Section 6, the results of the analysis provided evidence that there is not always a consistent relationship between wholesale sales and the business cycle. In other words, the correlation between wholesale sales and the business cycle varies depending on macroeconomic conditions, various government policies, or exogenous shocks.

In summary, based on our new and useful analytical framework for empirical study on wholesale sales, we highlighted characteristics of dynamic structure in the wholesale sales sectors in Japan and demonstrated the dynamic relationships between the wholesale sales for each business type and business cycles. The insights gleaned from this study offer valuable guidance for economists, policymakers, and investors navigating wholesale markets amid fluctuating economic conditions. Robust modeling techniques like DFDL modeling prove indispensable in capturing the nuanced dynamics inherent in these relationships, thereby informing strategic decision-making processes.

The research presented in this study holds significance for several reasons. First, we demonstrated a method to decompose time series data into components, facilitating the analysis of their structural changes. This approach enables a deeper understanding of the underlying dynamics within the data, unveiling trends, patterns, and anomalies that may not be readily apparent when examining the data as a whole. Moreover, we developed a modeling approach to analyze the dynamics in the relationship between variables. By in-

tegrating time-varying coefficients and the DFDL models, we could capture the evolving nature of relationships between variables over time, providing a more comprehensive analysis compared to static modeling approaches. Furthermore, our study represents a pioneering effort in rigorously analyzing the dynamic structure of wholesale sales. Through the application of the DFDL modeling approach and sector-specific analysis, we offer insights into the complex relationships between wholesale sales and business cycles. This novel approach holds significant implications for various empirical studies, offering a refined understanding of the dynamics of wholesale markets and their interactions with the broader economy.

A challenging aspect for future research is the statistical analysis and discussion concerning results such as component decomposition or the distribution of estimated time-varying coefficients. Further exploration in these areas could enhance the depth of understanding and contribute to the advancement of analytical methodologies in this field.

While the methods developed in this study inherently possess extrapolation capabilities and can thus be extended to forecasting applications, several limitations should be acknowledged when considering their practical use. Because no explicit model or distribution is assumed for the remaining component, the estimated structure may become complex, requiring experimentation with alternative modeling strategies such as ARMA-type specifications. Moreover, the inherently time-varying nature of wholesale sales and related macroeconomic variables implies that additional methodological innovations will be needed to adapt the current framework for predictive purposes. Addressing these challenges represents an important direction for future research, where the analytical approach introduced here can be refined and extended to forecasting tasks.

Author Contributions: K.K. played a role in the following points and made academic contributions: conceptualization, literature investigation, model construction, examination of analytical methods, estimation, interpretation of results, project administration, and writing (original draft and editing). H.N. played a role in the following points and made academic contributions: conceptualization, literature investigation, model construction, data curation, examination of analytical methods, estimation, interpretation of results, funding acquisition, and writing (original draft and editing). All authors have read and agreed to the published version of the manuscript.

Funding: This work was supported in part by a Grant-in-Aid for Scientific Research (C) (20K01639) from the Japan Society for the Promotion of Science.

Data Availability Statement: The dataset for Japan's wholesale sales value is available from Japan's Ministry of Economy, Trade, and Industry (https://www.meti.go.jp/english/statistics/index.html, accessed on 1 May 2023). The dataset for Japan's coincident CI is available from the website of Economic and Social Research (https://www.esri.cao.go.jp/en/stat/di/di-e.html, accessed on 1 May 2023) within the Cabinet Office of the Japanese government.

Acknowledgments: The authors gratefully acknowledge the anonymous reviewers for their constructive comments and suggestions, which have made this article more valuable and readable. An earlier version of this article was presented at the 2024 Japanese Joint Statistical Meeting, Tokyo University of Science, September 2024. We would like to thank participants at the 2024 Japanese Joint Statistical Meeting for constructive comments and suggestions.

Conflicts of Interest: The authors have no relevant financial or non-financial interests to disclose.

References

1. Wang, G. An analysis of the impact of sudden events on China's automobile industry stock price. *Asian J. Soc. Sci. Stud.* **2017**, *2*, 140–147. [CrossRef]
2. Noda, H.; Kyo, K. Do commercial sales move coincidentally with business cycles in Japan? A dynamic two-mode regression approach. *Appl. Econ. Lett.* **2019**, *26*, 1058–1066. [CrossRef]

3. Gupta, B.G.; Gaurav, A.; Panigrahi, P.K. Analysis of retail sector research evolution and trends during COVID-19. *Technol. Forecast. Soc. Change* **2003**, *194*, 122671 . [CrossRef] [PubMed]
4. Box, G.E.P.; Jenkins, G.M.; Reinsel, G.C. *Time Series Analysis: Forecasting and Control*, 4th ed.; Wiley: Hoboken, NJ, USA, 2008.
5. Brockwell, P.J.; Davis, R.A. *Time Series: Theory and Methods*, 2nd ed.; Springer: New York, NY, USA, 1991.
6. Brockwell, P.J.; Davis, R.A. *Introduction to Time Series and Forecasting*, 3rd ed.; Springer: New York, NY, USA, 2016.
7. Kitagawa, G.; Gersch, W. A smoothness priors state-space modeling of time series with trend and seasonality. *J. Am. Stat. Assoc.* **1984**, *79*, 378–389.
8. Kitagawa, G. *Introduction to Time Series Modeling with Application in R*, 2nd ed.; Chapman and Hall: London, UK, 2020.
9. Kitagawa, G.; Gersch, W. A smoothness priors time varying AR coefficient modeling of nonstationary time series. *IEEE Trans. Autom. Control* **1985**, *AC-30*, 48–56. [CrossRef]
10. Adeosun, O.A.; Olayeni, R.O.; Tabash, M.I.; Anagreh, S. Revisiting the Oil and food prices dynamics: A time varying approach. *J. Bus. Cycle Res.* **2023**, *19*, 275–309. [CrossRef]
11. Shi, S.; Hurn, S.; Phillips, P.C. Causal change detection in possibly integrated systems: Revisiting the money-income relationship. *J. Financ. Econom.* **2020**, *18*, 158–180. [CrossRef]
12. Kyo, K.; Noda, H.; Kitagawa, G. Co-movement of cyclical components approach to construct a coincident index of business cycles. *J. Bus. Cycle Res.* **2022**, *18*, 101–127. [CrossRef]
13. Kyo, K.; Kitagawa, G. A moving linear model approach for extracting cyclical variation from time series data. *J. Bus. Cycle Res.* **2023**, *19*, 373–397. [CrossRef]
14. Kyo, K. Enhancing business cycle analysis by integrating anomaly detection and components decomposition of time series data. *Stat. Methods Appl.* **2025**, *34*, 129–154. [CrossRef]
15. Harvey, A.C. *Forecasting, Structural Time Series Models and the Kalman Filter*; Cambridge University Press: Cambridge, UK, 1989.
16. Scott, S.L.; Varian, H.R. Predicting the present with Bayesian structural time series. *Int. J. Math. Model. Numer. Optim.* **2013**, *5*, 4–23. [CrossRef]
17. Clevel, R.B.; Clevel, W.S.; McRae, J.E.; Terpenning, I. STL: A seasonal-trend decomposition procedure based on loess. *J. Off. Stat.* **1990**, *6*, 3–73.
18. Findley, D.F.; Monsell, B.C.; Bell, W.R.; Otto, M.C.; Chen, B.-C. New capabilities and methods of the X-12-ARIMA seasonal-adjustment program. *J. Bus. Econ. Stat.* **1998**, *16*, 127–152. [CrossRef]
19. Kyo, K.; Noda, H.; Fang, F. An integrated approach for decomposing time series data into trend, cycle and seasonal components. *Math. Comput. Model. Dyn. Syst.* **2024**, *30*, 792–813. [CrossRef]
20. Akaike, H. A new look at the statistical model identification. *IEEE Trans. Autom. Control* **1974**, *AC-19*, 716–723. [CrossRef]
21. Kyo, K. Reinforcing moving linear model approach: Theoretical assessment of parameter estimation and outlier detection. *Axioms* **2025**, *14*, 479. [CrossRef]
22. Ito, T.; Hoshi, T. *The Japanese Economy*, 2nd ed.; The MIT Press: Cambridge , MA, USA, 2020.
23. JCA (Japan Cooperative Alliance). Survey Results on Consumer Behavior Regarding Agricultural and Livestock Products: Fiscal Year 2020 Survey. 2021. Available online : https://www.japan.coop/wp/wp-content/uploads/2020/03/200313_01.pdf (accessed on 1 May 2023). (In Japanese)
24. Noda, H.; Kyo, K. Dynamic relationships among changes in prices of beef, pork, and chicken in Japan: A Bayesian approach. *J. Agric. Food Res.* **2023**, *11*, 100464. [CrossRef]
25. Noda, H.; Osano, Y. Investment policies to extend the life of expressways in Japan. *Discret. Dyn. Nat. Soc.* **2017**, *2017*, 4296250. [CrossRef]
26. Kyo, K.; Noda, H.; Kitagawa, G. Bayesian analysis of unemployment dynamics in Japan. *Asian J. Manag. Sci. Appl.* **2013**, *1*, 4–25. [CrossRef]
27. Girardin, E. Growth-cycle features of East Asian countries: Are they similar? *Int. J. Financ. Econ.* **2005**, *10*, 143–156. [CrossRef]

Disclaimer/Publisher's Note: The statements, opinions and data contained in all publications are solely those of the individual author(s) and contributor(s) and not of MDPI and/or the editor(s). MDPI and/or the editor(s) disclaim responsibility for any injury to people or property resulting from any ideas, methods, instructions or products referred to in the content.